Discrete Voss surfaces: Designing geodesic gridshells with planar cladding panels

Nicolas Montagne, Cyril Douthe, Xavier Tellier, Corentin Fivet, Olivier Baverel

Discrete Voss Surfaces: Toward the design of Geodesic Gridshells

Nicolas MONTAGNE*[a,b], Cyril DOUTHE[a], Xavier Tellier[a], Corentin FIVET[b], Olivier BAVEREL[a]

* [a] Laboratoire Navier, UMR 8205, Ecole des Ponts, IFSTTAR, CNRS, UPE
77455 Champs-sur-Marne – MLV Cedex 2 – France
nicolas.montagne@enpc.fr

[b] EPFL, ENAC, Structural Xploration Lab, Passage du Cardinal 13b CH-1700 Fribourg

ABSTRACT

The design and construction of doubly-curved structures often reveals to be challenging and can result in complex manufacturing and assembly. A recent strategy to tackle this difficulty consists in exploiting the connection between discrete differential geometry and constructive properties to identify curve networks with good fabrication or mechanical properties. Following this approach, a family of surfaces, called Voss surfaces, is here presented. Among other features, they can be built from flat panels, initially flat straight strips, and hinged connections. These properties arise from the existence of a conjugate network of geodesic curves. Two generation methods are presented to shape discrete Voss surfaces: the first allows their exploration through linear spaces; the second provides a unique solution by means of a direct computation.

Keywords: Voss surface; Geodesic gridshell; Architectural geometry; Space exploration; Chebyshev net

1 INTRODUCTION

Building envelopes are a key aspect of the materialization of architectural intents. The recent advent of computer graphics opened the door to more complex, free-form shapes in architecture, and thus challenged conventional strategies of structural design and construction. Irregularly-curved geometries introduce new design issues that are not encountered with traditional spatial structures, often leading to fabrication and construction aberrations. For example, the use of triangulated networks to adapt target shapes often results in unique beam members and intricate nodal arrangements. On the other side, alternative non-triangular patterns do not ensure the possibility of a covering with flat panels. In this respect, bending-active structures are particularly appealing for their capacity to smoothly render freeform shapes and ease their fabrication [1]. Their members are elastically bent into a target position, and, together, form a network of curved elements fitting a doubly

curved surface. Furthermore, the erection process may contribute to the good mechanical behaviour of the system when the pre-stressing effect of bent members stiffens the structure.

A remarkable family of bending-active structures are elastic gridshells [2,3]. These structures are assembled flat on the ground from initially straight beams connected with simple rotational joints, and then erected into a target curved shape. The erection of the structure as a whole is permitted by a special arrangement of the beams into a regular grid, known as Chebyshev net. Elastic gridshells illustrate both the advantages and the difficulties faced when dealing with active-bending systems. Although, they create lightweight and large spanning support structures from elements that are easy to manufacture and assemble, their design also presents many issues. The actual geometry and the mechanical behaviour of elastic gridshells is hard to predict since it is given by the static equilibrium of the beam network and that members are largely-deformed and interconnected in dense layouts. In addition, members, generally wooden laths with rectangular cross sections, are subject to severe local stresses since the layout is imposed by the use of a Chebyshev net [4,5]. Additionally, the covering of the support structure usually requires custom curved panels, which reveals to be expensive and difficult to construct, or tailor-made fabric elements which assume a perfect control of the geometry and an increased maintenance.

1.1 Related Works

Research responding to the challenges raised for the design of elastic gridshells also proved useful for the more general field of active-bending structures. Past and current developments address various design aspects from geometric fitting, to numerical simulation of mechanical behaviour, envelope design and structural optimization.

From a geometrical point of view, the problem of mapping a given layout, namely a Chebyshev net, on an input target surface is a main focus. The IL team in Stuttgart pioneered the so-called compass method and hanging chain models to form-find the geometry of grids on given surfaces [6]. Bouhaya et al [7] addressed the same problem by projection and later optimized the positioning using genetic algorithms [8]. Alternatively, Lafuente Hernández et al. [9] proposed a methodology to design with an approximate Chebyshev net, while Masson [10] proposed solutions to introduce and manage singularities in the net. Sageman-Furnas et al. [11] gathered these different approaches in a single framework.

On a numerical modelling level, the capacity to simulate and evaluate the mechanical behaviour of bending-active structures has been greatly improved by the development of special numerical methods like dynamic relaxation [12]. Combined with the use of discrete element models, dynamic relaxation allows the quick and reliable assessment of equilibrium states and stresses in structures.

Since the initial development of the discrete element with three degrees of freedom accounting for axial stresses and bending [13], more complete formulations have been proposed to improve the precision of the model [14–18]. In contrast, Douthe et al. [19] evaded the problem of excessive stresses in members imposed by the Chebyshev net layout by using circular hollow cross section beams, hence avoiding torsion and improving bending compliancy. This approach proved to be conclusive in other works [5,20]. Other types of bending-active systems were also investigated mechanically [1].

Although bending-active structures and more specifically elastic gridshells have regained interest at the beginning of this century, their construction remains rare. This can be explained by the difficulty to cover these systems with envelopes, which has not much been addressed in research. In this regard, Schober and Schlaich [22] pioneered the use of translational net to ensure the covering of the structure with flat quadrangular panels. Recently, Douthe et al. [23] studied the special case of isoradial surfaces. The particularity of these manifolds is that they can be mapped by a Chebyshev grid and covered with planar faces. In geometry, it was found that conjugate nets of curves on smooth surfaces have a discrete equivalent: meshes with planar quadrilateral faces [24]. Since grid support structures are modelled as nets on surfaces, this property can be applied to ensure a covering of the structure with flat quadrilateral panels. In the case of isoradial surfaces, the interesting cladding property is due to the duality of the Chebyshev net with the conjugate net of principal curvature lines.

On another aspect, the problem of designing active bending with rectangular laths was not solved in the case of elastic gridshells but only wisely avoided by using an alternative cross section. Inspired by the precursory work of J. Natterer [25], Pirazzi and Weinand [26] propose an interesting solution for the design of bending-active shells with rectangular laths by using geodesic lines. Geodesic lines on surfaces have a vanishing geodesic curvature, therefore, a lath following such a line will not bend sideways. Since the slender element is not bent along its strong axis, severe stresses are avoided, as well as local instabilities. A geodesic line corresponds to the natural path of such elements on surfaces. Geodesic patterns on surfaces were further studied by Pottmann et al. [27]. The mapping of curved surfaces is addressed using several families of geodesic lines. Rabinovich et al. [26,27] used a special case of geodesic net, namely orthogonal geodesic nets, to model, deform, and explore the shape space of developable surfaces. In relation with the erection process of Chebyshev nets, Soriano et al. [30] as well as Pillwein et al. [31] explored the design of geodesic shells that can be constructed from an initially flat grid of laths. Wang et al. [32] used a similar notion, referred to as geodesic parallels to map surfaces with piecewise initially-flat strips.

In conclusion, various strategies for designing complex shaped envelopes can be found within the scope of bending-active systems. In particular, geodesic shells allow to build structures with

rectangular cross-sections tangent to the target surface. However, much like elastic gridshells, the lack of covering solutions with flat panels is a major limitation and contribute to a low uptake of such shells.

1.2 OVERVIEW

This paper studies the generation and transformation of discrete Voss surfaces, a special family of surfaces, whose geometrical properties ease fabrication and construction processes of freeform shells and gridshells. Voss surfaces were introduced and defined by Aurel E. Voss in 1888 [33] in their smooth version as surfaces that can be mapped by a conjugate network of geodesics. In their discrete version, Voss surfaces are meshes with flat quadrilateral faces whose opposite angles between edges at each vertex are equal [34]. Architectural envelopes based on discrete Voss surfaces can be built from regular elements despite their freeform shape. In particular, discrete Voss surfaces support the construction of geodesic gridshells, but can also be applied to flexible shell formworks [35] made of quadrangular flat panels, and assembled with simply-hinged connections. In the case of geodesic gridshells, they allow the use of initially-straight rectangular-cross-section beams without sideways bending, and covered with flat panels.

In section 2, the representation of discrete *Voss nets*, i.e. conjugate geodesic nets carried by Voss surfaces, through normal vectors is studied. This approach, inspired by existing studies on smooth cases, provides a dual shape encompassing all necessary constraints characterizing Voss nets. Then, in section 3, transformations are introduced to characterize the domain of possible shapes. Particular families of transformations enable the geometric alteration of Voss nets while maintaining their good constructive properties. In section 4, the above-mentioned characteristics are used for the generation of meshes from a relevant family of surfaces, namely Chebyshev nets on the unit sphere $\mathcal{S}^2$. More accurately, the shape space of Chebyshev nets on $\mathcal{S}^2$ creates a linear space of discrete Voss surfaces. The linear space is then used in section 5 to investigate and deform Voss surfaces using well-chosen transformation modes. This methodology addresses the design of surfaces from an exploratory point of view. A more straightforward method is then described, in which Voss surfaces are built from two boundary curves. Finally, applications of these techniques are exposed in section 6. Resulting doubly-curved shapes illustrate the large potential of discrete Voss surfaces for architectural applications.

1.3 NOTATIONS

The remainder of this paper focuses on meshes with planar quadrilateral faces. In this context, a general mesh, a mesh with planar faces and a planar quad mesh (so-called PQ mesh) will be denoted respectively by the script letters $\mathcal{M}$, $\mathcal{P}$ and $\mathcal{Q}$. Similarly, $\mathcal{V}$ will refer to a Voss net. Meshes are defined

by their list of vertices $(\mathrm{v}_i)_{i\leq I}$, of edges $\left(\mathrm{e}_j\right)_{j\leq J}$ and of faces $(\mathrm{f}_k)_{k\leq K}$ where the size of these lists are respectively I, J, K. The vertices of the mesh are stored in a column vector $\boldsymbol{V}$ of size $3I$, where matrixes will be distinguished by the use of bold capital letters. Therefore, $\boldsymbol{V}$ is given by:

$$\boldsymbol{V}^T = \left[\mathrm{v}_{1,x}, \mathrm{v}_{1,y}, \mathrm{v}_{1,z}, \mathrm{v}_{2,x}, v_{2,y}, \dots, \mathrm{v}_{I,y}, v_{I,z}\right]$$

Specific notions are introduced to qualify planar quad meshes. The vertex-star refers to the configuration depicted on Figure 1 - left and the face-star to the configuration on Figure 1 - right. Notations on these figures will be used in the following to depict the neighbourhood of vertices and faces. Vertices (Figure 1 - left), respectively faces (Figure 1 - right), on opposite sides of a vertex, respectively a face, have the same index. One is underlined, the other is not. Indices of a face in the neighbourhood of a vertex v (Figure 1 - left) are equivalent to the indices of the two other vertices bounding that face. The same is true when swapping vertices and faces (Figure 1 - right). Additionally, the affiliation to a mesh will be denoted in exponent when needed.

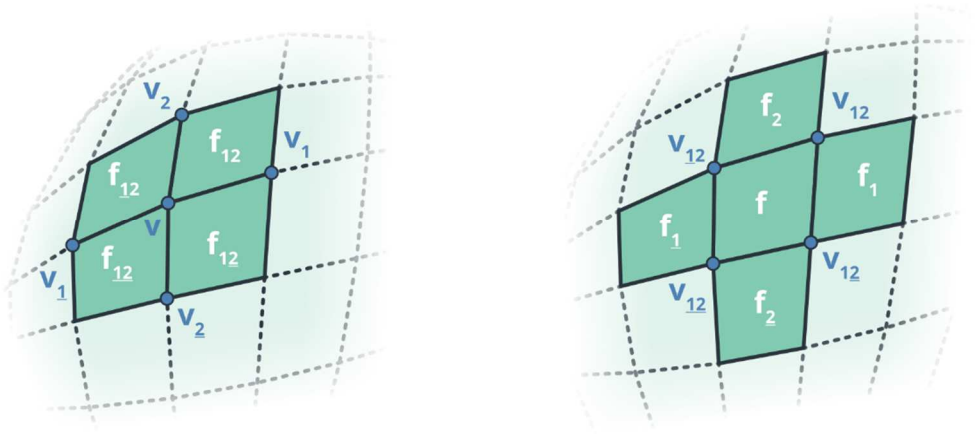

Figure 1: Illustration and naming convention for a vertex-star (left) and a face-star (right)

2 GAUSS MAP OF DISCRETE VOSS NETS

In the domain of classical differential geometry, a prolific strategy to extract properties of a surface is to study the variation its normal vectors. Its importance is highlighted by the central notion of Gauss Map. With $\mathcal{S}$ an orientable smooth surface, the Gauss map is the application that associates to each unit normal vector of $\mathcal{S}$ a point on the unit sphere $\mathcal{S}^2$, producing a new surface on $\mathcal{S}^2$. The study of

this application has proven useful to characterize and represent smooth varieties like developable surfaces.

The discrete counterpart of the Gauss Map is equivocal and subject to discussion. Indeed, when addressing polygonal meshes, the set of normal vectors can be defined upon several entities, i.e. the faces, the edges, or the vertices. Thus, different notions of Gauss maps can be defined, as long as they are consistent with one another. The relevance of a Gauss map is evaluated from the image produced on the unit sphere $\mathcal{S}^2$ and its capacity to characterize the underlying mesh. For example, Pottmann et al. [36] established a definition of Gauss map in the context of parallel meshes in which normals vectors are determined by comparing a pair of parallel meshes $\mathcal{P}$ and $\mathcal{P}'$. The normal vectors are defined by unitizing the distance between the corresponding vertices of $\mathcal{P}$ and $\mathcal{P}'$. This formulation proves to be relevant to analyse offset properties of support structures.

When it comes to planar quadrilateral meshes, a variety of options exists to determine normal vectors. The following sub-sections detail two of them that prove to be particularly relevant and complementary when dealing with discrete Voss surfaces.

2.1 DEFINITION FROM FACE NORMALS

Since discrete Voss nets are meshes with planar faces, a first way to determine normal vectors on the mesh builds on the faces' normals.

Definition 1: Let $\mathcal{Q}$ be a planar quad net, the Gauss map, or spherical projection of $\mathcal{Q}$ is the application which maps each normal vector of the faces of $\mathcal{Q}$ to the corresponding point on the unit sphere $\mathcal{S}^2$.

In the remainder, the Gauss map $\mathcal{G}$ designates either this application or the resulting mesh on $\mathcal{S}^2$ without ambiguity. As a consequence of the definition, the image of the Gauss map $\mathcal{G}$ is topologically dual to the initial mesh $\mathcal{Q}$ (Figure 2): every face, edge, or vertex of $\mathcal{Q}$ is transformed respectively to a vertex, edge or face of $\mathcal{G}$. This relation is reciprocal: every face, internal edge, internal vertex of $\mathcal{G}$ is respectively transformed to a vertex, edge, face of $\mathcal{Q}$.

The above definition of the Gauss map is actually more general than just the context of PQ meshes, and can be used to represent any mesh $\mathcal{P}$ with planar faces.

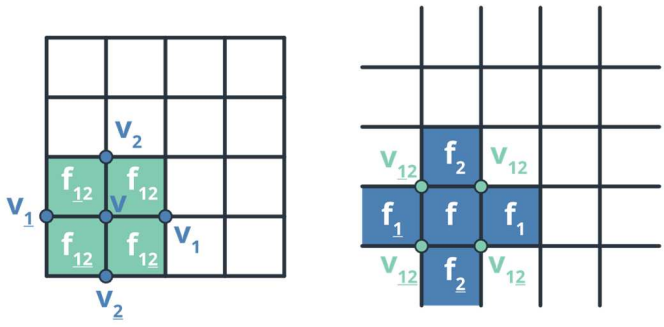

Figure 2: Schematic representation of the dual relation between a PQ net $\mathcal{Q}$ (left) and its Gauss map $\mathcal{G}$ (right).

It follows a first property on the projection of the angles made by edges around a vertex-star [37]:

Property 1: Let $\mathcal{Q}$ be a planar quad net, $\mathcal{G}$ its Gauss map, and the angles α_{12}, $\alpha_{\underline{12}}$, $\alpha_{\underline{12}}$, $\alpha_{\underline{12}}$ around the vertex v *of $\mathcal{Q}$, at a vertex-star. Let also β_{12}, $\beta_{\underline{12}}$, $\beta_{\underline{12}}$, $\beta_{\underline{12}}$ be the angles of the face* f *of $\mathcal{G}$, dual to* v*, at the vertices* n_{12}, $n_{\underline{12}}$, $n_{\underline{12}}$, $n_{\underline{12}}$*, dual to the faces* f_{12}, $f_{\underline{12}}$, $f_{\underline{12}}$, $f_{\underline{12}}$ *in $\mathcal{Q}$ (Figure 3). By construction, the spherical projection implies that the angles α_{12}, $\alpha_{\underline{12}}$, $\alpha_{\underline{12}}$, $\alpha_{\underline{12}}$ are transformed to their supplementary angles β_{12}, $\beta_{\underline{12}}$, $\beta_{\underline{12}}$, $\beta_{\underline{12}}$ respectively:*

$$\beta_{12} = \pi - \alpha_{12}, \qquad \beta_{\underline{12}} = \pi - \alpha_{\underline{12}}, \qquad \beta_{\underline{12}} = \pi - \alpha_{\underline{12}}, \qquad \beta_{\underline{12}} = \pi - \alpha_{\underline{12}}.$$

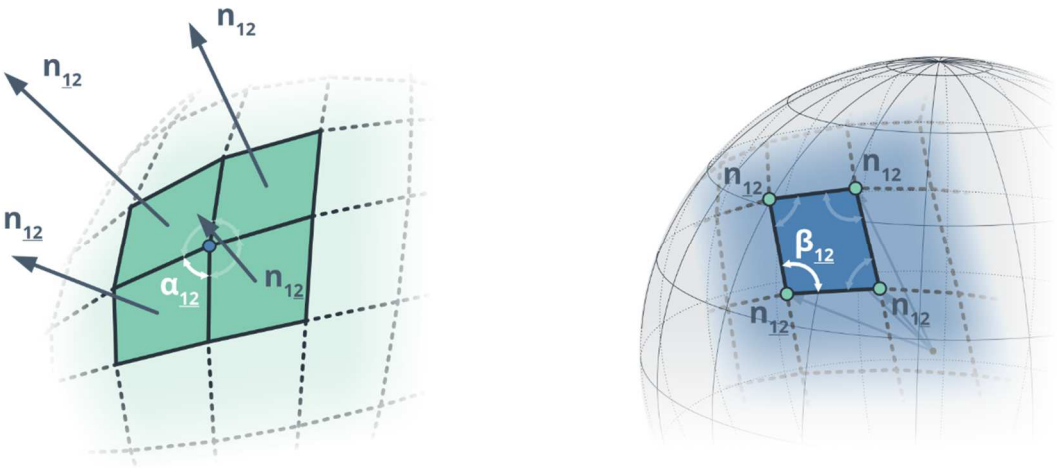

Figure 3: Spherical projection of a vertex-star. Angles around a vertex (left) are transformed to supplementary angles in the dual face of the Gauss map (right).

As an immediate consequence of the spherical projection of angles around a vertex, the faces of the Gauss map $\mathcal{G}$ of $\mathcal{V}$, a Voss surface, have equal opposite angles too. Thus, since $\mathcal{G}$ is a net on the unit sphere, the faces of $\mathcal{G}$ are spherical parallelograms (Figure 5). This is the defining property of discrete Chebyshev nets, which implies the essential characteristic of Voss nets [34]:

Property 2: Let $\mathcal{V}$ be a discrete Voss surface. The Gauss map of $\mathcal{V}$ is a Chebyshev net on the unit sphere $\mathcal{S}^2$, and will be denoted by $\mathcal{C}$.

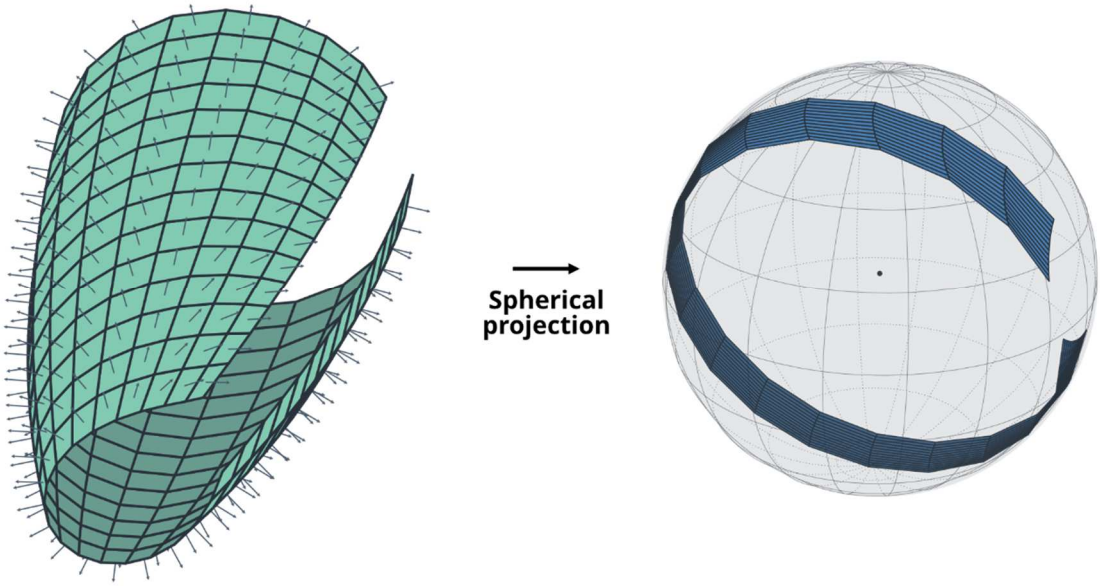

Figure 4: An example of a Voss net (left) and its Gauss Map (right)

As a consequence, any discrete Voss surfaces $\mathcal{V}$ is associated with a unique Chebyshev net $\mathcal{C}$ on the sphere $\mathcal{S}^2$ (Figure 4). The exact smooth counterpart of this property was stated in the founding article by A. Voss [33].

In this paper, a *discrete Chebyshev net* refers to a quad mesh whose faces are parallelograms on the surface. Therefore, the faces of a discrete Chebyshev net have equal opposite angles but also equal opposite edge lengths. On $\mathcal{S}^2$, since the curvature is constant, it is possible to rightfully replace the smooth notion of arc length with the discrete notion of length. Some papers make a distinction between regular Chebyshev and weak (or generalized) Chebyshev nets [38]. In the first case all edges of the quad mesh have equal length, while it is not necessarily true in the second case for which the length equality only stands for opposite edges in each faces. In 2D, the distinction segregates nets whose faces are all sheared squares in the first case or sheared rectangles in the second. The remainder of this paper considers the more general case of weak Chebyshev nets.

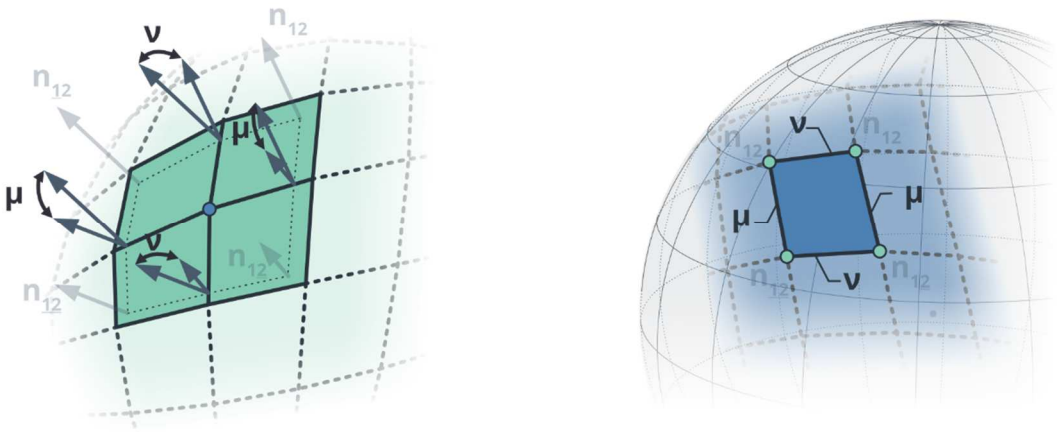

Figure 5: Spherical projection of dihedral angles of a discrete Voss net (left) onto its Gauss map (right), on which dihedral angles corresponds to the arc length of edges.

Since the Gauss map of a Voss net $\mathcal{V}$ is a Chebyshev net, the dihedral angles correspond to the angles made by the normal vectors of two adjacent faces. Because the length of opposite edges of a face of $\mathcal{C}$ are equal, the duality between $\mathcal{C}$ and $\mathcal{V}$ suggests that in both direction of the PQ mesh $\mathcal{V}$, dihedral angles are constant along each parameter line (Figure 5). According to Schief et al. [39], this property on dihedral angles can be taken as an alternative definition for discrete Voss surfaces. Thus:

Property 3: Let $\mathcal{P}$ be a planar quadrilateral net and $\mathcal{G}$ its Gauss map on the unit sphere. If $\mathcal{G}$ is a Chebyshev net on $\mathcal{S}^2$, then $\mathcal{P}$ is Voss net.

2.2 DEFINITION FROM VERTEX NORMALS

An alternative choice of normal vectors, described upon the vertices, can be found interpreting PQ meshes as discrete parametrizations of smooth surfaces. The notions of tangent and normal vectors to a curve need to be presented first. If C is a regular, non-degenerate curve at arc length s_1, i.e. $C'(s_1)$ and $C''(s_1)$ are non-null, then it is possible to compute the Frenet frame $(\mathrm{t}_1, \mathrm{n}_1, \mathrm{b}_1)$ at s_1, in which t_1 is the tangent vector, n_1 the normal vector and b_1 the binormal vector [40]. A discrete analogous definition exists for non-degenerate discrete curves, i.e. polylines for which any three consecutive vertices are not aligned:

Definition 2: Let P be a non-degenerate polyline and p_{i-1}, p_i, p_{i+1} three consecutive vertices of P (Figure 6 - *left). The Frenet frame of P at p_i, is designated by* $(\mathrm{t}_i, \mathrm{n}_i, \mathrm{b}_i)$, *where:*

$$\delta \mathrm{p}_{\underline{i}} = \mathrm{p}_{i-1} - \mathrm{p}_i, \qquad \delta \mathrm{p}_i = \mathrm{p}_{i+1} - \mathrm{p}_i,$$

$$\mathrm{t}_i = \frac{\delta \mathrm{p}_i - \delta \mathrm{p}_{\underline{i}}}{\left\| \delta \mathrm{p}_i - \delta \mathrm{p}_{\underline{i}} \right\|}, \qquad \mathrm{n}_i = \frac{\delta \mathrm{p}_i + \delta \mathrm{p}_{\underline{i}}}{\left\| \delta \mathrm{p}_i + \delta \mathrm{p}_{\underline{i}} \right\|}, \qquad \mathrm{b}_i = \mathrm{t}_i \wedge \mathrm{n}_i.$$

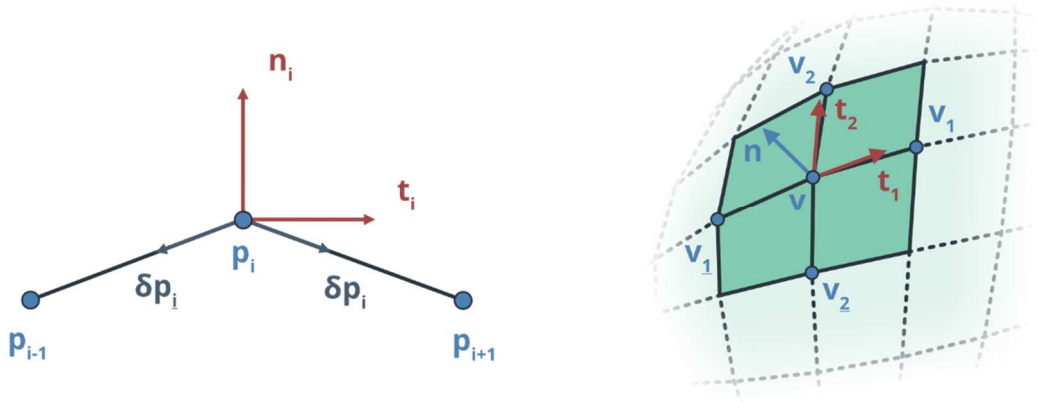

Figure 6: Frenet frame of a non-degenerate polyline (left) and mesh normal vector at a vertex computed from the tangent vectors of the coordinate-lines (right).

As mentioned above, PQ meshes define a two-way grid in space. It is thus possible to compute two Frenet frames (t_1, n_1, b_1) and (t_2, n_2, b_2) in both directions at a vertex-star v (Figure 6 - right). With t_1 and t_2 the tangent vectors at vertex v, the normal vector at the vertex is defined by:

$$n = \frac{t_1 \times t_2}{\|t_1 \times t_2\|}. \qquad (1)$$

This definition imitates the smooth case: with C_1 and C_2 two curves on a surface, intersecting at a point v, and t_1, t_2 the tangent vectors of these curves at v, the normal of the surface at v is aligned with the cross product of the tangent vectors t_1 and t_2.

For discrete geodesic nets, and therefore for Voss nets, Rabinovich et al. [28] showed that, just like in the smooth case, the normal vectors of two intersecting discrete geodesic curves agree at their intersection, meaning at their common vertex. As a consequence, the common normal vector of the curves coincides with the normal n in equation (1). Rabinovich et al. [28] used this result to define an adapted set of normals upon the vertices for the Gauss map of discrete orthogonal geodesic nets.

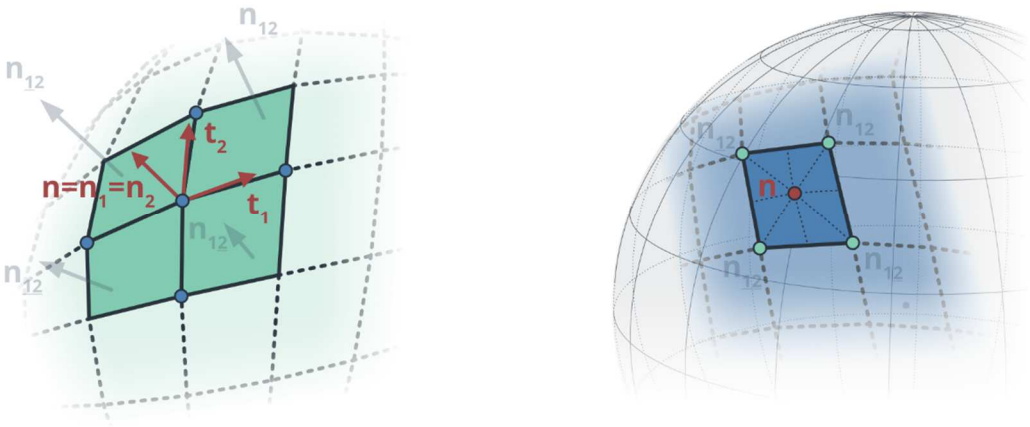

Figure 7: Projection of a normal at a node in a Voss net (left) onto its Gauss Map (right)

As a matter of fact, it is possible to identify this set of normal vectors defined upon the vertices in the Gauss Map of discrete Voss nets (Figure 7).

Property 4: Let $\mathcal{V}$ be a discrete Voss net and $\mathcal{C}$ its Gauss Map. Let's consider a vertex-star configuration and its spherical projection on $\mathcal{S}^2$.Thus, the face's normal $\mathrm{n}_{12}^{\mathcal{V}}$, $\mathrm{n}_{\underline{12}}^{\mathcal{V}}$, $\mathrm{n}_{\underline{12}}^{\mathcal{V}}$, $\mathrm{n}_{\underline{12}}^{\mathcal{V}}$ around the vertex v *of $\mathcal{V}$ are dual to $\mathrm{n}_{12}^{\mathcal{C}}$, $\mathrm{n}_{\underline{12}}^{\mathcal{C}}$, $\mathrm{n}_{\underline{12}}^{\mathcal{C}}$, $\mathrm{n}_{\underline{12}}^{\mathcal{C}}$ the vertices of $\mathcal{C}$, belonging to the face* f*, dual to* v*. The normal vector* n *at the vertex* v *of $\mathcal{V}$ corresponds on $\mathcal{S}^2$ to the centre of the spherical parallelogram* f*.*

The centre of the spherical parallelogram can be defined alternatively as the centre or intersection of its diagonals, or as the centre or the intersection of its medians [41] (id non vidi). This connection between the two notions of Gauss map, upon faces and vertices, enriches significantly the representation of discrete Voss surfaces on the unit sphere. The Chebyshev net on the unit sphere not only provides information on the face normals but also on the vertex normals of the Voss net.

3 TRANSFORMATIONS OF VOSS NETS

The study of mesh transformation is a very active field in geometry processing. Editing a mesh by prescribing displacements [42], or by using adapted subdivision patterns has been explored in many different situations and different paradigms compete.

A common method for mesh editing operates handle-based transformations: the user controls a small set of vertices and drags them around. Following these modifications, a new shape is computed after the resolution of an optimization problem [40,41]. Another method for editing polyhedral meshes operates constraint-based transformations: a given smooth surface is approximated by a mesh on which geometric constraints are defined [45]. The constraints, prescribed upon the vertices or the faces, express the geometrical behaviour expected for the tangential mesh. In practice this method tends to be time consuming and the resulting mesh only loosely respects the constraints [43,44].

Recently, an alternative approach has been proposed by Vaxman et al. [48] for polyhedral meshes and meshes with planar faces and has later been generalized by Poranne et al. [49]: polyhedral meshes and their transformation are described as linear spaces. The advantage of this method is that only exact solutions are explored in the process, which, on the other hand means that the design space is smaller than the previous methods. In [48], the shape space allows affine transformations of faces. Inspired by this approach, family of meshes, addressed as linear space, have been used in different contexts such as the design of planar quadrilateral meshes [50], and the form-finding of a shell-nexorade hybrid [51]. Pottmann et al. [36] address the linear space of parallel meshes for other reasons. This approach will be of particular interest in our context as well.

In this section, transformations that do not alter the defining attributes of discrete Voss nets are identified. The aim is to simplify the exploration of the shape space of Voss nets by using the point of view of meshes as linear spaces.

3.1 ISOMETRIC TRANSFORMATIONS

Isometric transformations have been a primary concern in discrete differential geometry during the past decade. In simple terms, they are defined as distance-preserving transformations. Their study is highly related to research on developable surfaces and on the exploration of deployable systems. Discrete isometric transformations are extensively used in origami for it preserves the length of the edge and only "folds" the mesh along these edges, and not at all faces.

Schief et al. [39] provide a thorough mathematical study on infinitesimal isometric transformation of discrete nets which reveals that discrete Voss surfaces admit a one-parameter family of isometric transformation that preserve their defining properties. Therefore, given a discrete Voss surface $\mathcal{V}$, it is possible to append the overall shape of the net without changing the edge length. In fact, only the dihedral angles of the mesh are modified. The transformation is ruled by the following relation (Figure 8):

$$tan\left(\frac{\mu}{2}\right) tan\left(\frac{\nu}{2}\right) = \frac{\sin(\alpha+\beta)}{sin(\alpha)+sin(\beta)}.$$

Keeping α and β constant, the isometric transformation of a discrete Voss surface is ruled by one parameter $r \in \mathbb{R}$:

$$\begin{cases} tan\left(\frac{\mu}{2}\right) \\ tan\left(\frac{\nu}{2}\right) \end{cases} \xrightarrow[r]{} \begin{cases} r \cdot tan\left(\frac{\mu}{2}\right) \\ \frac{1}{r} \cdot tan\left(\frac{\nu}{2}\right) \end{cases}.$$

In essence, the isometric transformation of Voss surfaces is determined by the choice of a single dihedral angle between two consecutive faces.

Tachi et al. [52] identified that generalized eggbox patterns in origami are discrete Voss surfaces. Indeed, opposite angles made by edges around each vertex are equal. For generalized eggbox patterns, the mesh corresponds to an alternation of valleys and mountain folds. It is this alternation that gives the bidirectional flat rigid-foldability property to the eggbox pattern. Mitchell et al. [53] made a connection between this rigid-foldability property of Voss surfaces and graphic statics, and used it to build a kinematic pavilion.

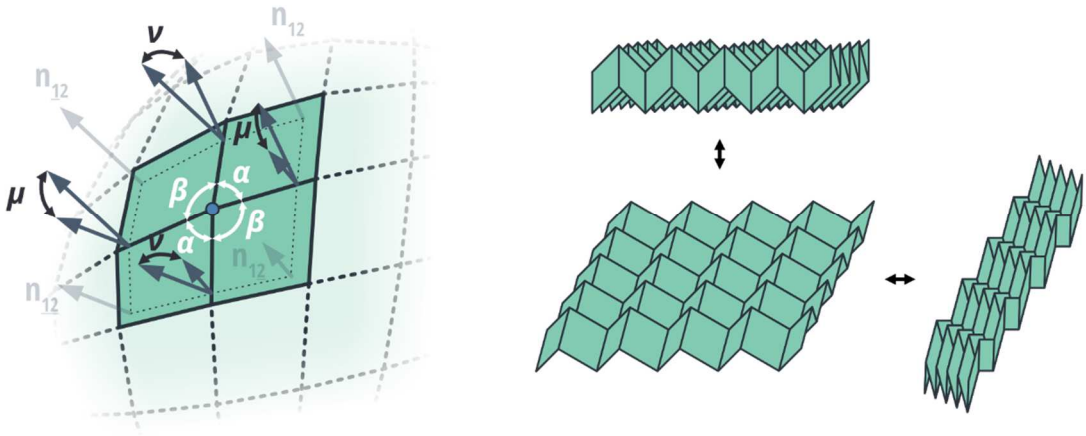

Figure 8: Angle properties of a Voss vertex-star (left); Folding motion of the eggbox pattern (right).

3.2 COMBESCURE TRANSFORMATIONS

Further essential examples of transformations are Combescure transformations. They are encountered for parallel meshes [36]. Two meshes are termed parallel if they have the same connectivity and if their corresponding edges are parallel. The transformation between two parallel meshes is called a Combescure transformation. Thus, given two parallel meshes $\mathcal{P}$ and $\mathcal{P}'$, with $(\mathrm{e}_j)_{j\leq J}$, $(\mathrm{e}'_j)_{j\leq J}$ their edges respectively, they respect the following linear relation:

$$\forall\, j \in J, e_j \times e'_j = 0$$

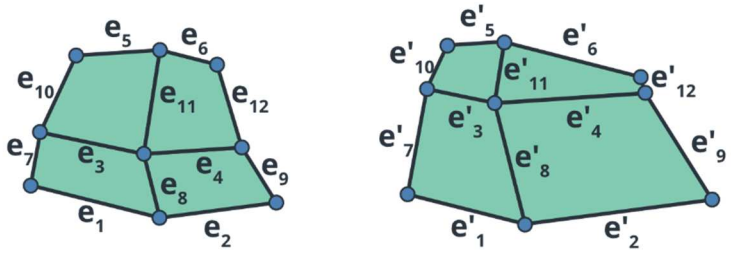

Figure 9: Two meshes related by Combescure transform.

Any planar quadrilateral net $\mathcal{Q}$ admits an infinite number of Combescure transforms. However, the dimension of the space of Combescure transforms $\mathfrak{C}_{\mathcal{Q}}$ of $\mathcal{Q}$ is finite and is combinatorically given by the following equation [36]:

$$\dim(\mathfrak{C}_{\mathcal{Q}}) = N_{\mathrm{e}} - 2N_{\mathrm{f}} + 3$$

where N_{e} is the number of edges in $\mathcal{Q}$, and N_{f} the number of faces in $\mathcal{Q}$. The dimension of the space of Combescure transforms must be understood as the number of degrees of freedom of the transformation. It represents the number of edge lengths that can be chosen within the mesh $\mathcal{Q}$, under the condition that all the constraints are compatible with one another. The number 3 at the end of the

equation stands for the global translations in the 3D Euclidean space, which leaves the edge length of the net unchanged.

If $\mathcal{P}$ and $\mathcal{P}'$ are two planar quadrilateral meshes, related by a Combescure transform, then their Gauss maps are identical. This results from the fact that by keeping edges parallel, the normal vectors of the faces remain unchanged. Therefore, Combescure transformations change Voss nets into other Voss nets, while preserving the Gauss map [39].

4 LINEAR SPACES OF VOSS NETS

The previous sections reviewed discrete surfaces whose geometric features are relevant for modelling shells from geodesic lines, with useful constructive and architectural properties – e.g. absence of sideways bending in rectangular cross-sections and covering with flat quadrilateral panels. The study highlighted remarkable properties, already known to geometers, notably on the Gauss map. Those properties are now used to set a methodology to identify appropriate design spaces of Voss surfaces.

4.1 REQUIREMENTS

The linear space of Voss nets is obtained after characterizing an appropriate shape space of quadrilateral meshes. This family of PQ meshes serves as the initialization for the creation of the linear space, in a similar fashion as proposed by Poranne et al. [49]. This ensures that the mesh, called a realization of the topology, always complies with the constraints used to create the linear space.

When identifying and computing a proper design space for Voss nets, the difficulty is to find the appropriate set of properties that corresponds to Voss nets. On the one hand, the number of constraints should be minimal: since explored shape spaces are already small in comparison with other non-linear methods, it is important to ensure that no potential member is missing out. On the other hand, constraints should not be too weak, in order to ensure that the linear space does not contain any mesh that is not a discrete Voss net. In addition to this, the design space exploration should be convenient.

4.2 ROLE OF THE GAUSS MAP

Following section 2, a relevant design space for discrete Voss nets is the Gauss map of this variety, namely the space of discrete Chebyshev nets on the unit sphere. In other words, the design of Voss nets is facilitated and guaranteed by starting from a Chebyshev net on $\mathcal{S}^2$.

Mimicking the behaviour of smooth Voss surfaces, all defining properties of discrete Voss nets are enclosed in their Gauss map and not more. Indeed, as stated, with $\mathcal{P}$ a planar quad net, and $\mathcal{G}$ its Gauss

map, if $\mathcal{G}$ is a Chebyshev net then $\mathcal{P}$ is a Voss net since the dihedral angles are constant along a coordinate-line. In addition, with the definition adopted for the spherical projection, it is always possible to define a planar quad net from a given mesh on the unit sphere (section 4.3). Hence, the Gauss map defines a surjection between the space of discrete Voss surfaces and the space of Chebyshev nets on the unit sphere. This demonstrates that the space of Chebyshev net on $\mathcal{S}^2$, representing the Gauss map of an underlying Voss net, is maximal.

However, for this space to be relevant for the design, it should allow a surjection from the space of Voss surfaces but also enable the exploration of all feasible discrete Voss surfaces. Further study into the inverse mapping is required.

4.3 COMPUTATION

In line with the previous section, the set of Chebyshev nets on $\mathcal{S}^2$, to be understood as the space of the Gauss maps of Voss nets, allows to narrow down the degrees of freedom for design exploration. For this manifold, the space of Gauss maps encloses just enough information, ensuring that the realization of the mesh will indeed be a Voss net. A construction of the linear space of Voss surfaces is provided in this section. More precisely, given an input Chebyshev net $\mathcal{C}$ on the unit sphere $\mathcal{S}^2$, the design space of Voss surfaces whose Gauss map is that input is characterized. Dealing with planar meshes, the following property holds:

Property 6: Let $\mathcal{P}$ be a mesh with planar faces, and e *an edge of $\mathcal{P}$ that does not lie on the boundary. Let* n_l *and* n_r *be the normal vectors of the faces adjacent to the edge* e*. Provided that* n_l *and* n_r *are not parallel,* $\mathrm{n}_l \times \mathrm{n}_r$ *is parallel to edge* e*, i.e.:*

$$(\mathrm{n}_l \times \mathrm{n}_r) \times \mathrm{e} = 0.$$

Considering the Gauss map of a net with planar faces, this property can be reformulated as follows:

Corollary 1: Let $\mathcal{P}$ be a mesh with planar faces and $\mathcal{G}$ its Gauss map. Let also $\mathrm{e}_i^{\mathcal{P}}$ *be an internal edge of $\mathcal{P}$ and* $\mathrm{e}_i^{\mathcal{G}}$ *the corresponding edge in $\mathcal{G}$ by the spherical projection. The normal vectors of the faces adjacent to* $\mathrm{e}_i^{\mathcal{P}}$ *correspond to the start vertex* $\mathrm{v}_{start}^{\mathcal{G}}$ *and the end vertex* $\mathrm{v}_{end}^{\mathcal{G}}$ *of the edge* $\mathrm{e}_i^{\mathcal{G}}$*. And thus* $\left(\mathrm{e}_{start}^{\mathcal{G}} \times \mathrm{e}_{end}^{\mathcal{G}}\right)$ *is parallel to the direction of* $\mathrm{e}_i^{\mathcal{P}}$*.*

As a consequence, the Gauss map encloses the direction of the edges of the underlying meshes. To simplify the discussion, the reconstruction of a single-face Voss net from the Gauss map is examined (Figure 10). Considering a Chebyshev net $\mathcal{C}$ reduced to only a vertex-star, the direction of the edges of the underlying face $\mathrm{f}^{\mathcal{V}}$ of $\mathcal{V}$, dual to the vertex $\mathrm{v}^{\mathcal{C}}$ of $\mathcal{C}$, are given by:

$$
\begin{aligned}
\mathrm{e}_1^{\mathcal{V}} &\parallel \left(\mathrm{v}_1^{\mathcal{C}} \times \mathrm{v}^{\mathcal{C}}\right) \\
\mathrm{e}_2^{\mathcal{V}} &\parallel \left(\mathrm{v}_2^{\mathcal{C}} \times \mathrm{v}^{\mathcal{C}}\right) \\
\mathrm{e}_{\underline{1}}^{\mathcal{V}} &\parallel \left(\mathrm{v}_{\underline{1}}^{\mathcal{C}} \times \mathrm{v}^{\mathcal{C}}\right) \\
\mathrm{e}_{\underline{2}}^{\mathcal{V}} &\parallel \left(\mathrm{v}_{\underline{2}}^{\mathcal{C}} \times \mathrm{v}^{\mathcal{C}}\right)
\end{aligned}
\qquad (2)
$$

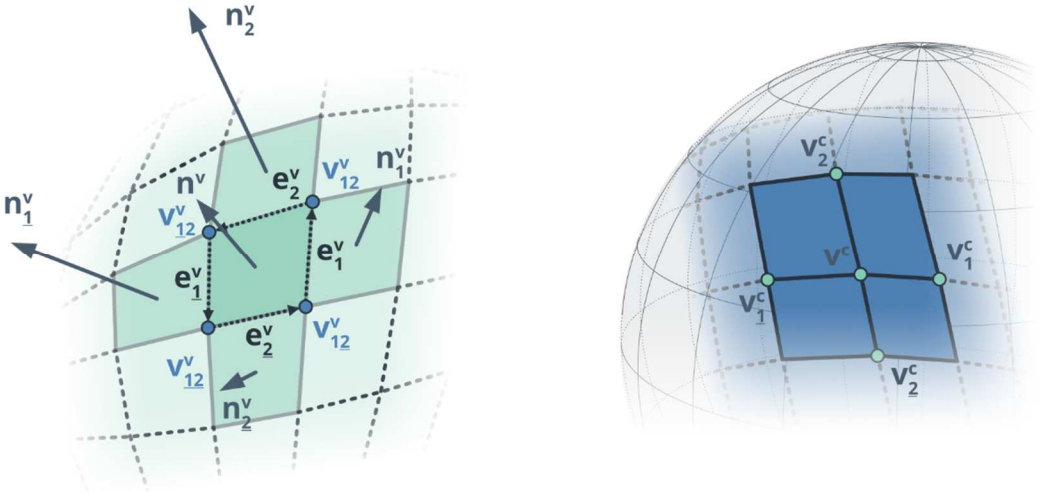

Figure 10: A Chebyshev net on the unit sphere (right) as the Gauss map $\mathcal{C}$ of a Voss surface $\mathcal{V}$ (left) to be determined. Edges $e_j^{\mathcal{V}}$ of $\mathcal{V}$, common to faces of normal $n^{\mathcal{V}}$ and $n_j^{\mathcal{V}}$ (left), are dual to edges $e_j^{\mathcal{C}}$ of $\mathcal{C}$, linking vertices $v^{\mathcal{C}}$ and $v_j^{\mathcal{C}}$ (right).

The directions of the edges are computed linearly upon the vertices of the Chebyshev net. However, recalling the notion of mesh parallelism, it is clear that having the information of the edge directions does not uniquely determine the face f. As illustrated in Figure 9, two distinct faces, related by a Combescure transform, can have parallel edges. With $\boldsymbol{V}_{\mathrm{f}}$ the column vector containing the coordinates of vertices $\mathrm{v}_{12}^{\mathcal{V}}$, $\mathrm{v}_{\overline{1}2}^{\mathcal{V}}$, $\mathrm{v}_{\overline{12}}^{\mathcal{V}}$, $\mathrm{v}_{1\overline{2}}^{\mathcal{V}}$ of face f, above relations (2) are rewritten:

$$
\begin{cases}
\left(\mathrm{v}_1^{\mathcal{C}} \times \mathrm{v}^{\mathcal{C}}\right) \times \left(\mathrm{v}_{12}^{\mathcal{V}} - \mathrm{v}_{1\overline{2}}^{\mathcal{V}}\right) = 0 \\
\left(\mathrm{v}_2^{\mathcal{C}} \times \mathrm{v}^{\mathcal{C}}\right) \times \left(\mathrm{v}_{\overline{1}2}^{\mathcal{V}} - \mathrm{v}_{12}^{\mathcal{V}}\right) = 0 \\
\left(\mathrm{v}_{\underline{1}}^{\mathcal{C}} \times \mathrm{v}^{\mathcal{C}}\right) \times \left(\mathrm{v}_{\overline{12}}^{\mathcal{V}} - \mathrm{v}_{\overline{12}}^{\mathcal{V}}\right) = 0 \\
\left(\mathrm{v}_{\underline{2}}^{\mathcal{C}} \times \mathrm{v}^{\mathcal{C}}\right) \times \left(\mathrm{v}_{12}^{\mathcal{V}} - \mathrm{v}_{\overline{12}}^{\mathcal{V}}\right) = 0
\end{cases}
\Rightarrow \boldsymbol{B}_{\mathrm{f}}(\mathcal{C}) \cdot \boldsymbol{V}_{\mathrm{f}} = 0
$$

The relation of edge parallelism is expressed linearly using the vertices of the face to rebuild, and a matrix $\boldsymbol{B}_{\mathrm{f}}$ which only depends on the vertices of $\mathcal{C}$. In this equation, the unknown is the column $\boldsymbol{V}_{\mathrm{f}}$, which contains the vertices of face f. Consequently, the null space $\mathrm{null}(\boldsymbol{B}_{\mathrm{f}})$ can be interpreted as the linear space containing all quadrilateral faces whose edges are parallel to the direction prescribed by the Gauss map $\mathcal{C}$.

Now, with $\mathcal{C}$, a more complex Chebyshev net, with several faces, the characterization of the underlying meshes $\mathcal{V}$, with several faces, relies on the generalization of matrix $\boldsymbol{B}_{\mathrm{f}}$. Computing all matrixes $\boldsymbol{B}_{\mathrm{f}}$

independently, for each face f of $\mathcal{V}$, using each vertex-stars of $\mathcal{C}$, the matrixes $\boldsymbol{B}_{\mathrm{f}}$ are combined in a single large matrix $\boldsymbol{B}$ of size $\left[3J^{\mathcal{V}} \times 3I^{\mathcal{V}}\right]$, which gives:

$$\boldsymbol{B}(\mathcal{C}) \cdot \boldsymbol{V} = 0$$

Where $\boldsymbol{V}$ is the column vector of the vertices of $\mathcal{V}$, interpreted as the combination of all $\boldsymbol{V}_{\mathrm{f}}$, and where $\boldsymbol{B}$ only depends on the vertices of $\mathcal{C}$. Consequently, $\mathrm{null}(\boldsymbol{B})$, defined only from $\mathcal{C}$, is the linear space of dimension N composed of meshes whose Gauss map is $\mathcal{C}$.

4.4 GEOMETRIC INTERPRETATION

The study of the reconstruction of meshes from a given Gauss map led to the definition of a linear space, described as the null space of a matrix. Therefore, the design of a Chebyshev net $\mathcal{C}$ on $\mathcal{S}^2$ leads to the definition of a linear space of Voss surfaces, only dependent on $\mathcal{C}$. Actually, the null space $\mathrm{null}(\boldsymbol{B})$, contains Voss nets that are all related by Combescure transforms. The elementary matrixes $\boldsymbol{B}_{\mathrm{f}}$ defined on the each face, help describing the space of quadrilateral face whose edges are parallel to directions given by the Gauss Map. Each $\mathrm{null}(\boldsymbol{B}_{\mathrm{f}})$ is the linear space of quad faces related by Combescure transforms respecting the constraints on the edges. Combining the face matrixes in a single matrix **B** guarantees that the constraints on the faces are geometrically compatible with one another, making sure that $\mathrm{null}(\boldsymbol{B})$ is not always reduced to zero. Therefore, $\mathrm{null}(\boldsymbol{B})$ is the linear space of meshes whose edge directions are prescribed by the initial Chebyshev net $\mathcal{C}$ on the unit sphere. They are related by Combescure transforms. From a mathematical perspective, the space of Chebyshev nets on $\mathcal{S}^2$ is in bijection with the quotient set of Voss surfaces under the equivalence relation of Combescure transformations.

Importantly, $\mathrm{null}(\boldsymbol{B})$ is never reduced to zero when the Chebyshev net is larger than a 2×2 complex of faces. A planar quad mesh, realization of the given Gauss Map, always exists by definition of the Gauss map.

Remarkably, the reconstruction of the linear space from a Gauss map presented above is very general. It can actually be applied for the characterization of general meshes with planar faces, since it mainly depends on the definition of the Gauss map as the projection on $\mathcal{S}^2$ of the normal of the face. Therefore, polygonal meshes with different types of faces can be studied in this way, as long as faces are planar. In our context, this approach proved to be particularly relevant since all and only defining constraints of discrete Voss surfaces are enclosed in their Gauss map.

5 GENERATION OF VOSS SURFACES

The design space for discrete Voss surfaces identified in section 4 is used for the generation of discrete Voss surfaces. Two different methods are presented. The first consists in exploring the linear space of discrete Voss surfaces (section 5.2). The second consists in a direct computation of the Voss net from two target boundary curves (section 5.3). Beforehand, section 5.1 exposes existing approaches to generate Chebyshev nets on surfaces.

5.1 GENERATION OF CHEBYSHEV NET ON THE SPHERE

The study of the space of Chebyshev nets on $\mathcal{S}^2$ is a preliminary to the generation of discrete Voss surfaces and has already been addressed in the literature.

Historically, Chebyshev introduced this variety of nets on smooth surfaces in 1878 for their capacity to approximate the behaviour of fabric around the human body. Such a net can be assembled initially as a flat two-way grid, and then its transformation approximates the behaviour of flexible but inextensible rods. Thus, Chebyshev nets can be found in various contexts, such as stylish furniture or medical stents. Its use for architectural venues, initiated by Frei Otto, resulted in the association of Chebyshev nets with the structural notion of elastic gridshells.

Mathematically, Chebyshev nets on a surface are defined by hyperbolic equation and their generation involves the solution of the Sine-Gordon equation [54]. The determination of such nets is therefore a problem of propagation. On this kind of problems, unique solutions are determined from the prescription of boundary conditions or from the propagation of an element. As exposed in section 1.1, the problem of mapping Chebyshev nets on given smooth surfaces has been addressed many times, geometrically and computationally. Unlike the case of elastic gridshells, where these nets directly model the support structures, Chebyshev nets are used here as a representation of Voss nets on the unit sphere. Thus, requirements on the net differ from usual applications, since smoothness is here not necessary. Still, similar generation methods can still be applied in our case, but the scope is reduced to the generation of Chebyshev nets on the unit sphere.

A first choice of generation method consists two primal boundary curves as initial conditions [10]. This process corresponds to the so-called “compass method” introduced by Otto et al. [6]. Let $P_a = (\mathrm{a}_i)_{i \leq A}$ and $P_b = (\mathrm{b}_j)_{j \leq B}$ be two polylines, whose starting vertices coincide. Recalling that a Chebyshev net is defined by equal opposite lengths in each face, it is possible to rebuild iteratively the parallelograms by starting from the intersection of P_a and P_b, and by using the subdivisions of both polylines. Parallelograms are computed line by line, or diagonally. The process stops when the $(\mathrm{A}-1)(B-1)$ quadrilateral faces are mapped.

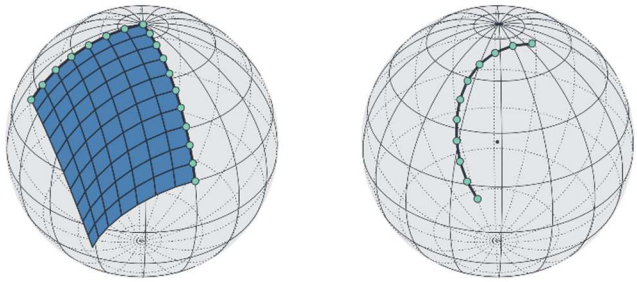

Figure 11: Chebyshev nets generated from two primal boundary conditions.

Figure 11 illustrates two examples of Chebyshev nets on the unit sphere generated from two primal boundary conditions. The primal conditions are the discretized lines, depicted by thicker lines. The parallelograms are successively computed from the intersection of the two lines to the opposite corner of the mesh. The situation on the right sphere is a degenerate case where one of the two lines is reduced to a point. Thus, the resulting Chebyshev net is curve. The underlying Voss net is in fact a developable net, mapped by a conjugate geodesic network. This is a well-known fact of differential geometry: all developable surfaces are indeed Voss surfaces.

A second choice consists in generating Chebyshev nets from secondary conditions denoted as "initial zigzag" [36,51]. This method relies on the initial prescription of the diagonal parallelograms of the Chebyshev net. Secondary conditions correspond to the vertices on a diagonal and to the next or previous diagonal line, which is equivalent to a zigzag (Figure 12). Similarly, the parallelograms are then computed diagonally, on one side and the other.

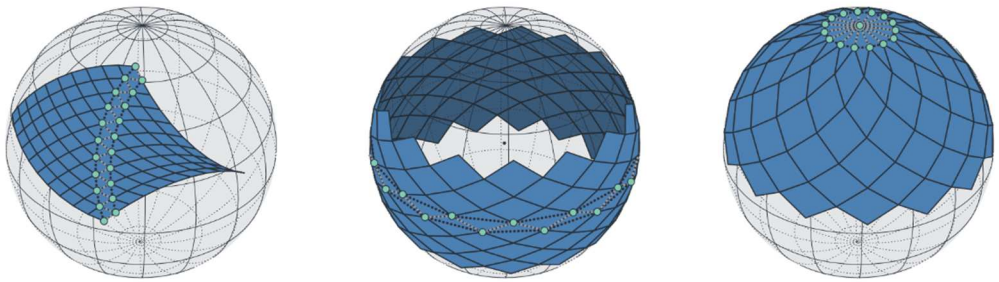

Figure 12: Chebyshev nets on the unit sphere generated from secondary conditions. Open (left) and closed (middle) polylines on $\mathcal{S}^2$ are used. The rosette condition (left) is a degenerate case.

Figure 12 shows three applications of this second generation method where the secondary conditions are represented with dotted lines. Open (left) and closed (middle) polylines are used as support for the secondary conditions, resulting respectively in an open and closed looping Chebyshev net on $\mathcal{S}^2$. The degenerate situations where one of the secondary curves is reduced to a point is also illustrated (right).

A third choice consists in mixing the two aforementioned boundary conditions (Figure 13 left).

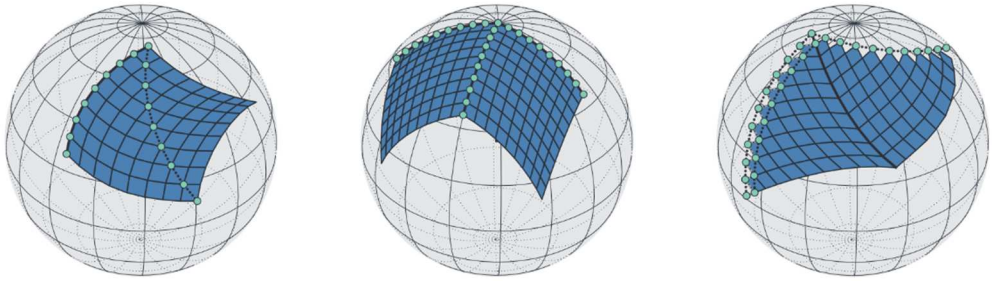

Figure 13: Examples of a mixed condition (left) and of patches of Chebyshev nets generated from primal (center) or dual (right) curves.

Masson studied the notion of patches or junction between Chebyshev nets [10]. The bounding polylines of a given Chebyshev net are seen as potential input curves for the generation of attached Chebyshev nets. This allows the mapping of surfaces that could not be approximated by a single Chebyshev net by defining several nets compatible with one another, in the sense that they match at their common polyline.

Figure 13 illustrates the patch of primal (center) and secondary (right) conditions. In the first case, the compatibility of the generated Chebyshev nets results from the use of a common boundary polyline. Regarding the patch of secondary conditions, only one secondary polyline is required to create the second Chebyshev net (on the right). The generation of this second net can also be seen as a mixed generation which uses the new boundary of the first Chebyshev net as a primal polyline.

The generation methods presented above always lead to a Chebyshev net. Depending on the situation addressed, one condition may be more relevant than another, in a similar way as for partial differential equations where the resolution is eased by the use of adapted initial conditions. The methods differ by their initial inputs for resolution. Depending on the problem addressed, one boundary condition may prove to be more relevant than another. For the generation of Voss nets, an arrangement of the grid on the boundary can turn out to be technically or architecturally more interesting. A methodology to compute the spherical parallelograms of Chebyshev nets on $\mathcal{S}^2$ by means of unit quaternions is presented in the Appendix: Computation of a Chebyshev net $\boldsymbol{\mathcal{S}^2}$.

5.2 Exploration of discrete Voss surfaces

As exposed in the previous section, a number of options exists to generate Chebyshev nets, supporting the choice made for a reduced design space for Voss surfaces. Following results from sections 4.3 and 4.4, once a Chebyshev net $\mathcal{C}$ is computed on $\mathcal{S}^2$, the matrix $\boldsymbol{B}$ is calculated upon the vertices of $\mathcal{C}$, and the linear space of $\mathrm{null}(\boldsymbol{B})$ is to explore.

Contrary to usual approaches, the starting point is not an initial mesh but its Gauss map, which is topologically dual. Therefore, best-fit algorithms comparing trial shapes with a target surface cannot

be directly be implemented in this context. Instead, the objective is to identify a basis of the linear space $\mathrm{null}(\boldsymbol{B})$ which allows its smooth and informed description.

EIGENSHAPES

Poranne et al. [49] suggested the use of eigenshapes to generate initial smooth meshes and transform them. Eigenshapes are defined as the eigenvectors of the Laplacian **L** of the mesh, a quadratic function. For each vertex v, the Laplacian gives a direction for the smoothing of the mesh, based on the neighbour vertices v_i of v:

$$\boldsymbol{L}(\mathrm{v}) = \mathrm{v} - \frac{1}{n}\sum_{i=1}^{n} \mathrm{v}_i$$

Eigenshapes, or eigenvectors of the Laplacian $\boldsymbol{L}$ constrained on $\mathrm{null}(\boldsymbol{B})$, form a special basis of the space $\mathrm{null}(\boldsymbol{B})$. Unlike a random basis of this linear space, each eigenshape corresponds to a smooth Voss surface. Alternatively, eigenshapes can also be seen as transformation modes if they are added to a realization of this space. Therefore, in the present case, eigenshapes serve for the generation of an initial Voss surface of $\mathrm{null}(\boldsymbol{B})$ and then for the transformation of this element. The best candidates for the initial realization are found by minimizing the Rayleigh quotient:

$$\min_{\boldsymbol{V} \,\epsilon\, null(\boldsymbol{B})} \frac{\boldsymbol{V}^T \cdot \boldsymbol{L} \cdot \boldsymbol{V}}{\boldsymbol{V}^T \cdot \boldsymbol{V}}$$

Since we are interested in applying transformations and thus in exploring the whole linear space described by $\mathrm{null}(\boldsymbol{B})$, the minimization problem is indirectly solved by finding the eigenvectors of $\boldsymbol{L}$. To account for the constraints of $\boldsymbol{B} \cdot \boldsymbol{X} = \boldsymbol{0}$, an orthonormal basis $\boldsymbol{N}$ of $\mathrm{null}(\boldsymbol{B})$ is computed by running a Singular Value Decomposition (SVD) on $\boldsymbol{B}$. Thus, every vector of $\mathrm{null}(\boldsymbol{B})$ can be written as $\boldsymbol{N} \cdot \boldsymbol{W}$ for some column vector $\boldsymbol{W}$. This also has the effect of reducing drastically the number of unknowns to N, the exact dimension of $\mathrm{null}(\boldsymbol{B})$ given earlier as the dimension of the space of Combescure transforms:

$$\min_{\boldsymbol{V} \,\epsilon\, null(\boldsymbol{B})} \frac{\boldsymbol{V}^T \cdot \boldsymbol{L} \cdot \boldsymbol{V}}{\boldsymbol{V}^T \cdot \boldsymbol{V}} \Leftrightarrow \min_{\boldsymbol{W}} \frac{\boldsymbol{W}^T \cdot \boldsymbol{N}^T \cdot \boldsymbol{L} \cdot \boldsymbol{N} \cdot \boldsymbol{W}}{\boldsymbol{W}^T \cdot \boldsymbol{W}}$$

The eigenshapes are then given by computing an eigenvalue decomposition of the matrix $\boldsymbol{N}^T \cdot \boldsymbol{L} \cdot \boldsymbol{N}$ and taking the eigenvectors of the resulting matrix. Consequently, the smoothest meshes of the linear space $\mathrm{null}(\boldsymbol{B})$ are the eigenshapes of $\boldsymbol{N}^T \cdot \boldsymbol{L} \cdot \boldsymbol{N}$ with the lowest eigenvalues. In the present case, this allows to define a smooth initial discrete Voss surface $\mathcal{V}$, whose Gauss map is the Chebyshev net $\mathcal{C}$ which was used to compute $\boldsymbol{B}$.

MINIMAL INFLUENCE MODES

Interpreting $\mathrm{null}(\boldsymbol{B})$ as a space of transformation modes for Voss nets, an alternative solution for the exploration of the linear space is to create a basis of modes with minimal influence on the overall geometry.

The formulation of such basis derives from the observation that given a planar mesh $\mathcal{P}$, the Combescure transformations of $\mathcal{P}$ sorts the edges of the mesh into groups of co-dependent edges. Thus, if an edge is stretched or shortened under a Combescure transformation, then all the other edges from its group are also modified. Combescure transformation form an equivalence relation on the edge of $\mathcal{P}$ and the number of equivalence class is $N-3$, living out the three global translations in space. For example, considering the simple case depicted on Figure 9, the equivalence class would be $[e_1] = \{e_1, e_3, e_5\}$, $[e_2] = \{e_2, e_4, e_6\}$, $[e_7] = \{e_7, e_8, e_9\}$, $[e_{10}] = \{e_{10}, e_{11}, e_{12}\}$. Taking one representative edge by equivalence class, the aforementioned basis of $\mathrm{null}(\boldsymbol{B})$ is composed of transformation modes which alter one of the representative while leaving the length of all the other selected edges unchanged.

The research of the modes is achieved on a reduced space $\boldsymbol{N_{reduced}}$ of size $\left[3I^{\mathcal{V}}_{reduced} \times N-3\right]$ obtained from $\boldsymbol{N} = \mathrm{null}(\boldsymbol{B})$, of size $\left[3I^{\mathcal{V}} \times N\right]$, by filtering the three global translations and then by keeping the line of the matrix correspond to the vertices involved at the start or the end of the representative edges. With $\boldsymbol{R}$ the matrix computing the edge vectors of the representatives from their start and end vertex coordinate in $\boldsymbol{N_{reduced}}$, the problem of finding the basis is equivalent to solving:

$$\forall i, 1 \leq i \leq N-3, \qquad \boldsymbol{R} \cdot \boldsymbol{N_{reduced}} \cdot \boldsymbol{X} = \boldsymbol{E_i}, \qquad where\ \boldsymbol{E_i} = [0 \cdots 1 \cdots 0]\ canonical\ vectors\ of\ E^{N-3}.$$

Finally, the $N-3$ solution vectors $\boldsymbol{X}$ are each multiplied by $\boldsymbol{N_{filtered}}$ in which the three global translations were previously filtered. This produces basis vectors on the whole space and not on the reduced one.

Compared with the eigenshapes, this alternative method to explore $\mathrm{null}(\boldsymbol{B})$ proved more intuitive for the transformation of already computed Voss net. The ability to only have local modifications revealed useful for the design of Voss nets as well as for patching them together.

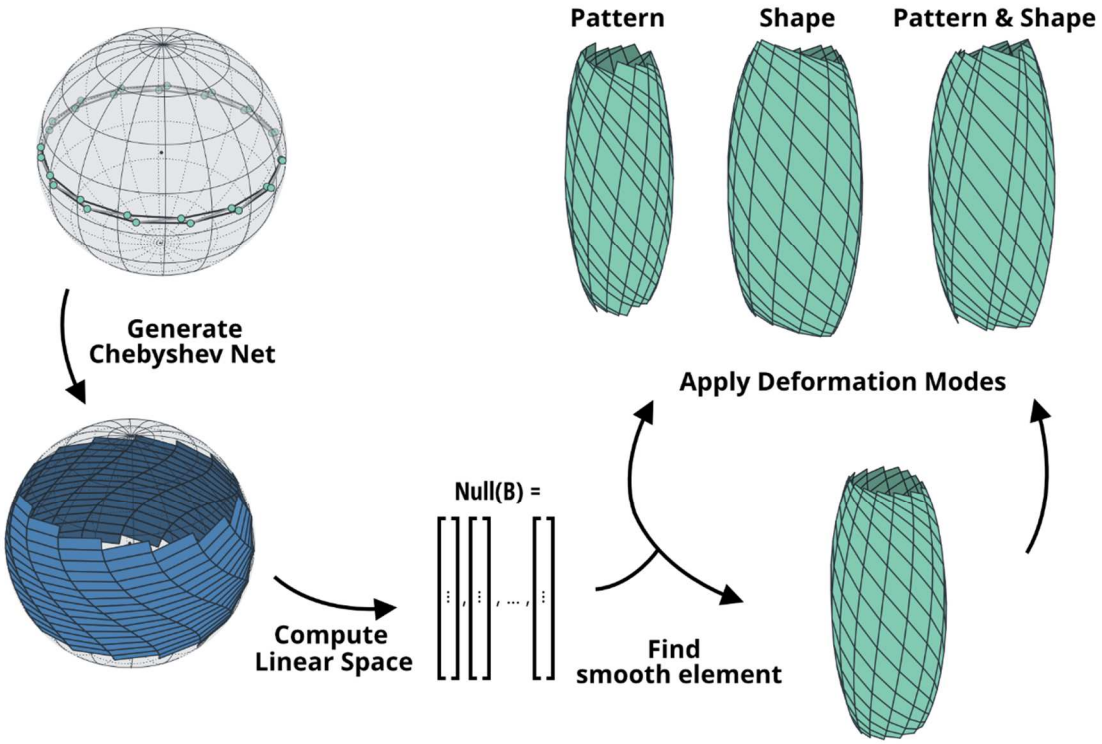

Figure 14: Process for the exploration of linear spaces of discrete Voss surfaces.

Thus, the entirety of $\mathrm{null}(\boldsymbol{B})$ can be explored by adding either eigenshapes or minimal influence modes to $\mathcal{V}$. The effect is the transformation of the mesh while keeping the Gauss map of $\mathcal{V}$ unchanged. These approaches give very satisfying solutions for closed and open meshes and allows to have relevant transformation modes (Figure 14), which is not the case when simply using an orthonormal basis of $\mathrm{null}(\boldsymbol{B})$.

5.3 Direct generation of discrete Voss surfaces

The methodology exposed in the previous section explores linear spaces of Voss surfaces, i.e. produces a variety of shapes. However, in some cases, one can be interested in a more explicit approach, i.e. in directly computing a discrete Voss surface from initial constraints expressed in the Euclidean space and not on the Gauss map. Therefore, a direct generation method is presented, which uses two boundary curves as input.

Let P_a and P_b be two polylines whose first vertices are coincident. These curves correspond to the boundary coordinate-lines of the Voss net to generate. Given that P_a and P_b are not degenerated, the Frenet frame at each internal vertex is computable. This is equivalent to interpreting the curves P_a and P_b as discrete geodesic lines on a surface. The Frenet frames give the normal vector at each internal vertex, which corresponds to the centre of each spherical parallelograms of the Gauss map. With this information only, there are some degrees of freedom left for the design of the Chebyshev net on $\mathcal{S}^2$. The missing information is to be found at the intersection of the input curves. Since P_a and P_b are the

boundary curves, their vertices $a_0 = b_0$, a_1 and b_1 are contained in the same planar facets at the starting corner. Therefore, the first vertices of the polylines give the normal vector of the initial facet. The Chebyshev net is then generated from the first face normal and the set of vertex normals (Figure 15).

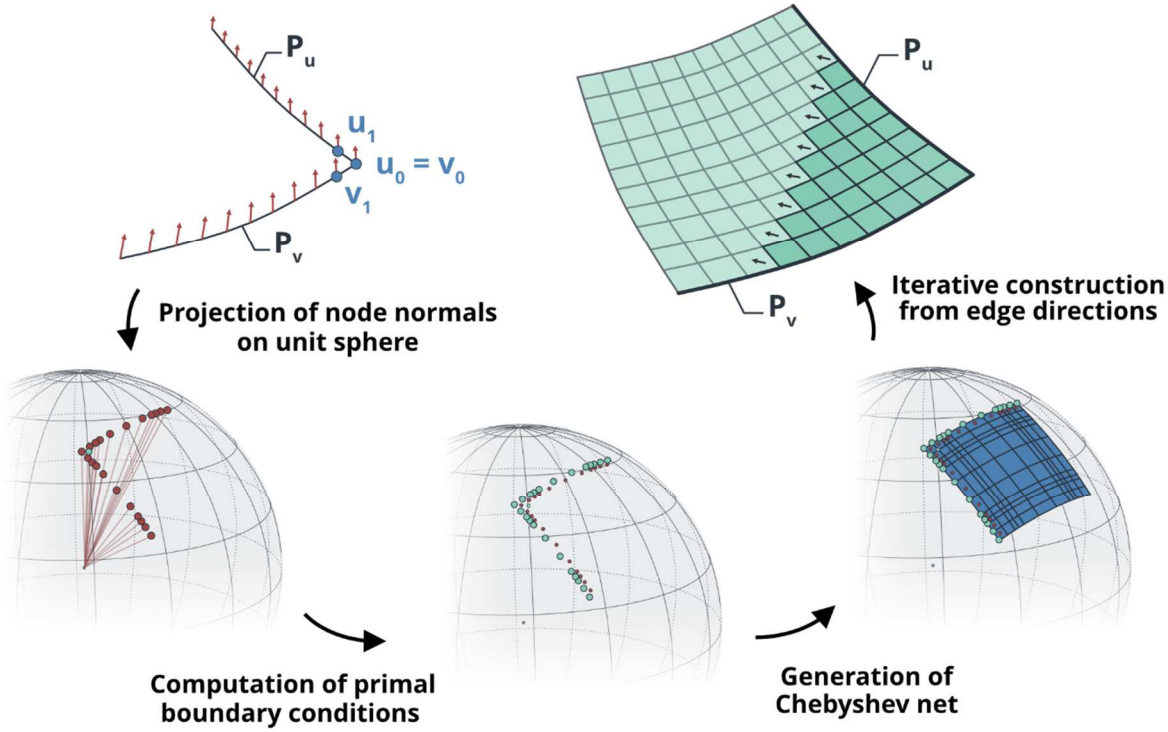

Figure 15: Process for the direct computation of discrete Voss surfaces

The Chebyshev net computed on the unit sphere gives access to the direction of each edge of the discrete Voss net to be constructed from the boundary curves. In relation with the previous generation method, a possible technique to construct the Voss net from there would be to compute the matrix $\boldsymbol{B}$ and the eigenshapes of the Laplacian, to describe $\mathrm{null}(\boldsymbol{B})$. Then, to find the unique solution that fits with the vertices of the boundary curves P_a and P_b, an additional linear system would have to be solved. Instead, a more straightforward approach is adopted. In order to reduce significantly computational time, constraints are solved locally, at the scale of the face and not globally on the mesh [56]. Considering v_a, v_b, v_c and v_d the vertices of a planar quad face of $\mathcal{V}$, and d_1, d_2, d_3 and d_4 the direction of the edge given by the Gauss map (Figure 16), if the length of two edges is known then it is possible to know the length of the two others by solving:

$$\begin{pmatrix} l_1 - l_4 \cdot \cos(\alpha) \\ l_4 \cdot \sin(\alpha) \end{pmatrix} = \begin{pmatrix} \cos(\beta) & -\cos(\alpha + \delta) \\ \sin(\beta) & \sin(\alpha + \delta) \end{pmatrix} \begin{pmatrix} l_2 \\ l_3 \end{pmatrix}$$

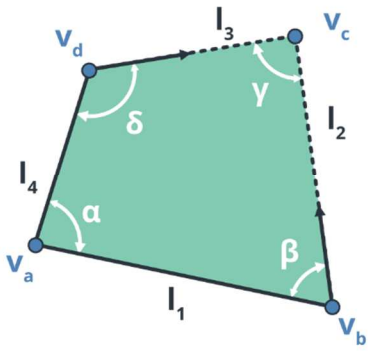

Figure 16: Computation of the last vertex of a planar face from two edge length.

Thus, the Voss net is given by iteratively computing the faces, starting at the intersection of the boundary discrete geodesic coordinate-line, in a similar way than for the Chebyshev net. In conclusion, the direct generation of the discrete Voss net is permitted by the extensive use of the different interpretations and analyses of the Gauss map presented in the preceding sections.

6 APPLICATIONS

The methodologies presented in the previous section are applied for the computation of doubly-curved shapes, all based on discrete Voss surfaces.

6.1 FORMAL EXPLORATION

The framework proposed gives access to a large variety of complex geometries. The design of discrete Voss surfaces with positive, negative or sign-changing Gaussian curvature is possible, although the design space, the unit sphere, has a constant positive Gaussian curvature.

The first methodology, based on the computation of a linear space, provides enough freedom to investigate diverse shapes and to alter them quickly. Interestingly, new shapes can be found from linear combinations of realizations, since the Voss nets are parts of the same linear space. Because the generation of Voss nets is done through an abstract representation, it requires a certain intuition to manipulate the Gauss Map. On the other hand, the determination of discrete Voss surfaces from two boundary curves reveals more intuitive. With this second method, the designer has an explicit and prompt way to build Voss nets.

Resorting to Chebyshev patches permits the concatenation of discrete Voss surfaces while ensuring continuity between them. In a similar fashion as for Chebyshev nets, using patches provides a mean to insert and manage singularities in the discrete Voss nets. Examples of constructions are compiled on Figure 17, where the separation between patches is denoted by thick black lines.

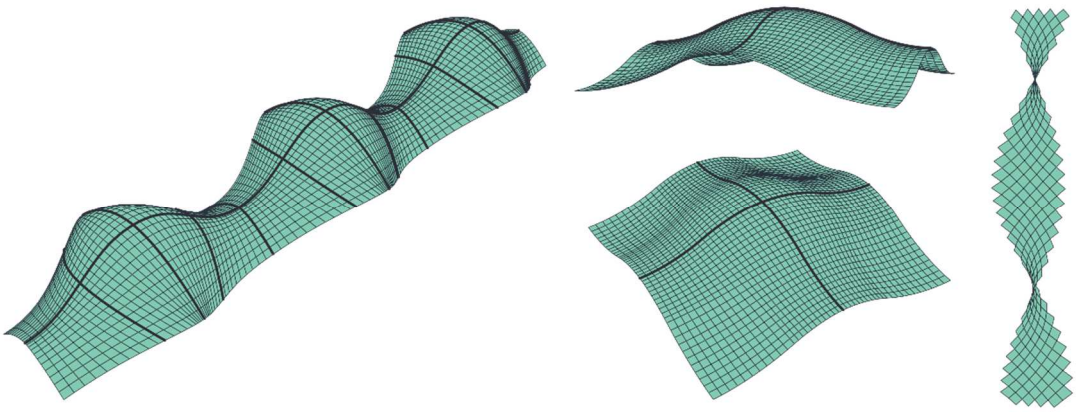

Figure 17: Discrete Voss surfaces generated from Chebyshev patches. Left: Geodesic gridshell inspired by the gridshell of Downland [3]. Center: Geodesic gridshell canopy which can be repeated in both directions. Right: Twisting periodic Voss net.

6.2 TRANSFORMATIONS

ISOMETRIC TRANSFROMATIONS

Isometric transformations are distance preserving transformations. As an extension of developable surfaces, discrete Voss nets admit a one-parameter family of isometric transformations. During such transformations, the shape of each face is kept identical, while their orientation varies in space. Consequently, given an initial Voss net, a family of meshes with same faces is deduced by prescribing one parameter for the transformation.

Figure 18 shows examples of discrete Voss surfaces related by isometric transformations. The different cases have been obtained by choosing the dihedral angle between two consecutives faces. The Gauss Map is then deformed accordingly.

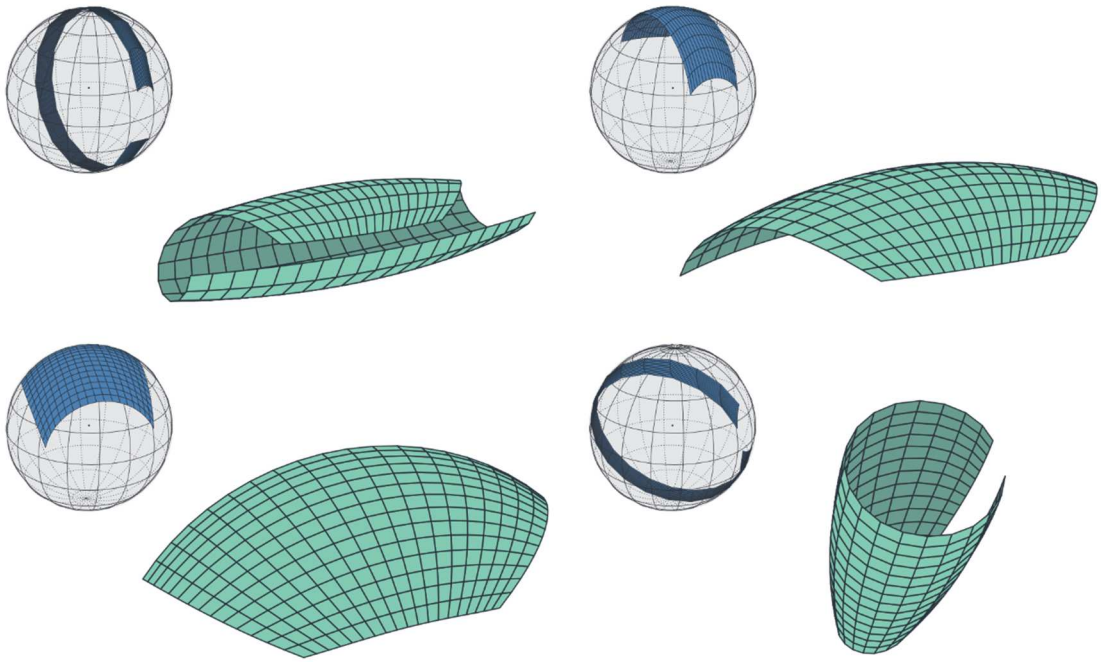

Figure 18: Discrete Voss surfaces related by isometric transformations.

COMBESCURE TRANSFORMATIONS

Furthermore, Combescure transformations also preserve the defining properties of discrete Voss surfaces. Here, they are applied to alter the geometry of Voss and explore the shape space. In Figure 19, the initial discrete surface with a positive Gaussian curvature (left) is transformed into a net with negative Gaussian curvature (right).

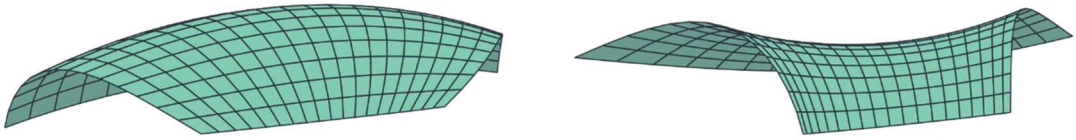

Figure 19: Voss surfaces with positive Gaussian curvature (left) and negative Gaussian curvature (right) both related by a Combescure transform.

6.3 SHAPE FITTING WITH VOSS NETS

The framework developed in this paper ensure that the surfaces drawn do not have approximate but the exact properties. This guideline led to the formulation of Voss nets as linear space but has evaded options such as ruled-based optimization, heavily used for fitting target shapes. However, the goal of fitting a target surface is not inherently incompatible with the work presented. In this subsection, illustrating the potential of our methodology, the fitting of a translational surface is studied (Figure 20 – left). The surface considered originates from an example given by Schober and Schlaich [22] and is obtained by translating a parabola along another orthogonal parabola. By cutting this surface with a circle, Schober and Schlaich were able to obtain a doubly curved dome that can be covered with flat

panels only, and which could have been implement in projects such as the Neckarsulm swimming pool cover.

For the shape-fitting optimization on this target surface S, an adapted linear space of Voss nets is first defined. Knowing the surface S, its Gauss map $\mathcal{G}$ is retrieved by projecting the normal vectors on the unit sphere. To ensure a complete covering of the Voss net $\mathcal{V}$ on the target S, the Gauss map $\mathcal{C}$ of $\mathcal{V}$ has to be greater than $\mathcal{G}$. In the case of the translational surface, a simple bi-symmetrical Chebyshev net $\mathcal{C}$ has been designed on $\mathcal{S}^2$ (Figure 20 – top). From this initial guess $\mathcal{C}$, the linear space $\mathrm{null}(\boldsymbol{B})$ and then the minimal influence modes were computed. For a mesh $\mathcal{V}$ of 17×17 faces, it resulted in 34 transformation modes of $\mathcal{V}$, to combine with the three global translation.

For practical reasons, the optimization method used is an implementation of the genetic algorithm called Galapagos [57]. The genotype is composed the 37 modes of transformation. The fitness function is composed of three parts: the first one sums the distance of each vertices of $\mathcal{V}$ to the target surface S to ensure closeness; the second enforces symmetricity on $\mathcal{V}$ by summing the length discrepancies among symmetrical edges , and the last energy aligns the meshes by weighting the distance between the in-plane projection of their barycentre. The respective weights of the parts are 1.0, 20 and 20.

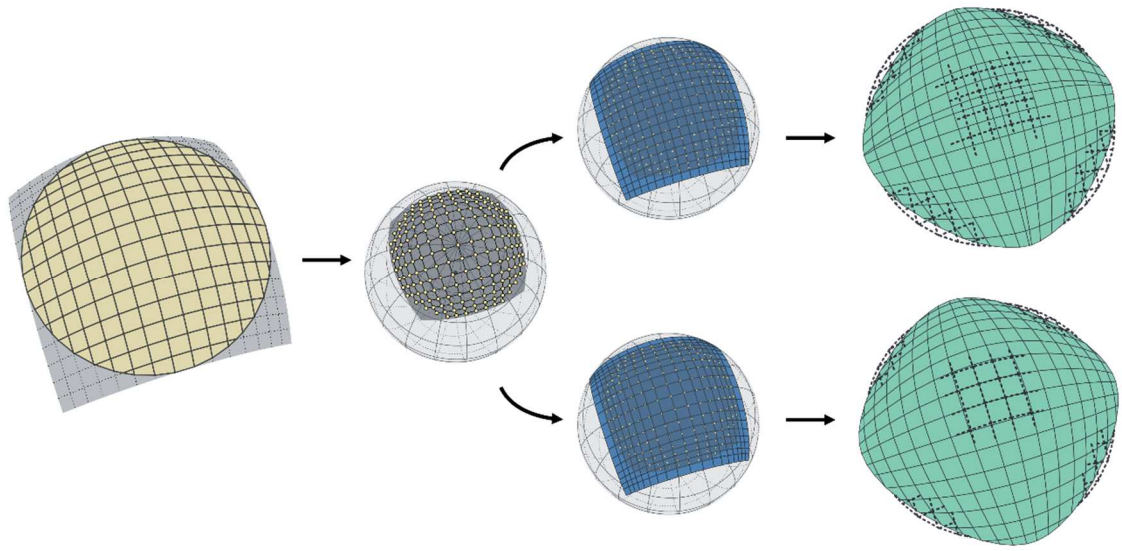

Figure 20: Step of the fitting optimization of a translational surface with a Voss net. On the right, the Voss net resulting from the optimization with the exceeding portions of target surface in dotted lines

After optimization, a first convincing result was obtained. The maximal and mean distances of the vertices of $\mathcal{V}$ to the target geometry are respectively about 2.5 % and 0.7% of the surface diameter. However the pattern of the Voss net looks uneven due to the fact that the Gauss map $\mathcal{C}$ was a regular Chebyshev net. To smoothen the division pattern of the net $\mathcal{V}$, edge length of the Chebyshev net could have been added in the genotype. This option assumes that the linear space has to be computed again

after each generation which is time consuming. Therefore, the Gauss map of $\mathcal{V}$ was altered manually to a weak Chebyshev and after few iterations, another conclusive Voss net was found (Figure 20 – bottom). On this result, the mean and max distances are similar with respectively 2.8% and 0.78% of the target surface diameter.

The advantage of using a linear space is that the optimization ran on only 37 parameters, while it would have been done on $3 \times I = 972$ values corresponding to the coordinate in space of each vertices of $\mathcal{V}$. On the other hand, the Voss nets resulting from the optimization fit the target geometry only approximately. The fact that the Gauss map has to be a Chebyshev net limits the shapes accessible to Voss nets.

6.4 CONSTRUCTIVE INTERPRETATION

In this section, the relation between Voss nets and their constructability as geodesic gridshells is illustrated through two examples. For such interpretation, the edges of the meshes represent discrete geodesic lines and are thus approximations of the path taken by rectangular cross-section beams. Similarly, the faces of the mesh correspond exactly to flat panels used for the covering of the support structure.

The first example is based on a Voss net with a positive Gaussian curvature (Figure 21 – top right). The simplicity of the geometry (Figure 21 – top right) allows to grasp the transition leading to the simulated layout of the rectangular cross section beams (Figure 21 – top middle) and then to a real mock-up (Figure 21 – top right). The real mock-up is made of organic glass beams with 1.5mm by 8mm rectangular cross sections, assembled together with earing connectors to enforce tangency of intersecting members. The overall geometry of the grid took form progressively while assembling the beams on by one.

The second case study comprises an arrangement of several Voss nets (Figure 21 – bottom left). The central net itself is a composition of Voss nets which generate a singularity at the top. Then, three identical branches are patched on the sides. To display the feasibility of the geometry, a model of the pavilion with a beam layout and panel thickness is exposed (Figure 21 – bottom right). The panel thickness is set to 100 mm to emphasise on the capacity of Voss net to adapt large thickness. After a preliminary sizing of the bent members based on their curvature, 8mm by 80mm rectangular cross-section laths are used in the gridshells. The beams at free borders of the branches are double in place to fix their geometry while the supports are better fixed than hinged. This guarantees the proximity of the surface model with the relaxed configuration of the gridshell, thus reducing the tolerances and improving the capacity to fix the rigid panels over the support structure.

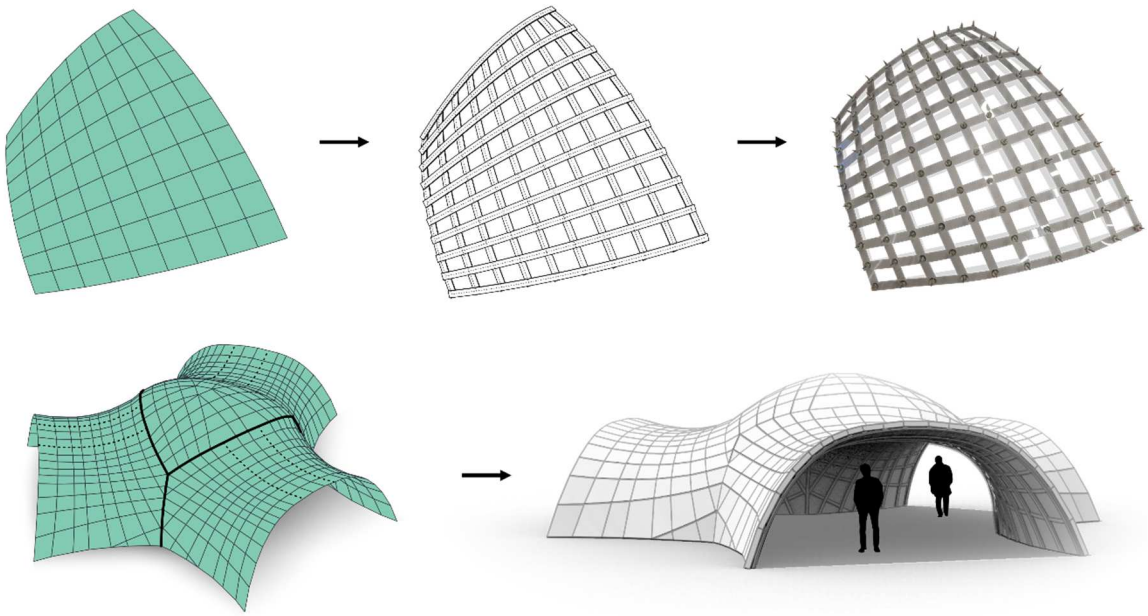

Figure 21: A composition of Voss surfaces with a singularity at the centre (top - left) along with its constructive interpretation which includes the flexible beam layout and the thickness of the covering panels (top - left); A simple Voss surface (bottom - left), with the expected beam layout (bottom - middle) and the built mock-up (bottom - right).

CONCLUSIONS

This paper addresses the design of geodesic gridshells, a family of shells that can be built from initially-straight beams arranged in a layout which avoids sideways bending, and that can be covered with flat quadrilateral panels only. These unique beneficial construction features are made possible by using discrete Voss surfaces and their unique geometrical properties.

A generation process is presented, which starts with the creation of a Chebyshev net $\mathcal{C}$ on the unit sphere, and interprets it as the Gauss map of Voss surfaces. The vertices of the Gauss map are used to compute edge directions and create a matrix, whose null space is a linear space containing all corresponding Voss surfaces. Smooth realizations of this space are obtained after computing a special basis of the null space, called eigenshapes, the best candidate being the eigenshapes associated with the lowest eigenvalue. The exploration of other realizations associated with the same Gauss map $\mathcal{C}$ is achieved at no computational cost by employing other eigenvectors or with minimal influence modes.

In addition, a process to directly compute Voss surfaces from two boundary curves is presented. It uses the normal at the vertices of the mesh and generates the unique underlying Voss surface in linear time.

Finally, applications comprise the generation of the best-fit discrete surface to a target mesh. The fitting is tackled from the Gauss map since it reduces the number of degrees of freedom for the optimisation process. Additional geometries are presented, including the model of a pavilion.

Further developments should address the mapping of a Chebyshev net on complex Gauss maps. Although several methods already deal with the approximation of surfaces with Chebyshev nets (section 1.1), Gauss maps often presents singularities and cusps, a problem that is not systematically addressed in the past proposed methodologies. In addition, the described generation strategies do not apply to the exploration of the developable surfaces subfamily, since the gauss map is reduced to a curve. Alternative methods can be formulated with more information than solely the Gauss map.

Following the research presented in this article, focused on the theoretical framework, a pavilion has been designed and built. Thus, the constructive details, the mechanical study of Voss nets, and the built structure will be presented in an upcoming article.

AUTHOR'S CONTRIBUTIONS

Nicolas Montagne developed the theoretical formalism in the paper with the help of Xavier Tellier regarding differential geometry and under the supervision of Cyril Douthe. Nicolas Montagne devised the mathematical interpretations, generation methodologies and their computational implementation with advices from Cyril Douthe. Nicolas Montagne wrote the manuscript in consultation with Cyril Douthe for the development. All the authors provided critical feedback all along the development of the research, and supervised the writing of the paper.

ACKNOWLEDGMENT

The authors warmly thank Romain Mesnil for the fruitful discussions on topics ranging from architectural geometry, to structural morphogenesis to implementation details, as well as Laurent Hauswirth for the enlightening advices in differential geometry. The authors also thank Arthur Lebée for valuable enlightenments in the domain of origami structures.

BIBLIOGRAPHY

[1] J. Lienhard, H. Alpermann, C. Gengnagel, and J. Knippers, 'Active Bending, a Review on Structures where Bending is Used as a Self-Formation Process', *International Journal of Space Structures*, vol. 28, no. 3–4, pp. 187–196, 2013, doi: 10.1260/0266-3511.28.3-4.187.

[2] E. Happold and W. I. Liddell, 'Timber lattice roof for the Mannheim Bundesgartenschau', *Structural Engineering*, vol. 53, no. 3, pp. 99–135, 1975.

[3] R. Harris, J. Romer, O. Kelly, and S. Johnson, 'Design and construction of the Downland Gridshell', *Building Research & Information*, vol. 31, no. 6, pp. 427–454, 2003, doi: 10.1080/0961321032000088007.

[4] G. C. Quinn and C. Gengnagel, 'A review of elastic grid shells, their erection methods and the potential use of pneumatic formwork', in *WIT Transactions on the Built Environment*, Belgium, 2014, vol. 136, pp. 129–144. doi: 10.2495/MAR140111.

[5] L. Du Peloux, F. Tayeb, O. Baverel, and J.-F. Caron, 'Construction of a Large Composite Gridshell Structure: A Lightweight Structure Made with Pultruded Glass Fibre Reinforced Polymer Tubes', *Structural Engineering International*, vol. 26, no. 2, pp. 160–167, 2016, doi: 10.2749/101686616X14555428758885.

[6] F. Otto, J. Hennicke, and K. Matsushita, *IL10 Gitterschalen*. 1974.

[7] L. Bouhaya, O. Baverel, and J.-F. Caron, 'Mapping two-way continuous elastic grid on an imposed surface: application to grid shells', in *IASS 2009: Evolution and Trends in Design, Analysis and Construction of Shell and Spatial Structures*, Valencia, 2009, pp. 989–998. Accessed: May 30, 2020. [Online]. Available: https://hal.archives-ouvertes.fr/hal-00531430

[8] L. Bouhaya, O. Baverel, and J.-F. Caron, 'Optimization of gridshell bar orientation using a simplified genetic approach', *Structural and Multidisciplinary Optimization*, vol. 50, no. 5, pp. 839–848, 2014, doi: 10.1007/s00158-014-1088-9.

[9] E. Lafuente Hernández, O. Baverel, and C. Gengnagel, 'On the Design and Construction of Elastic Gridshells with Irregular Meshes', *International Journal of Space Structures*, vol. 28, no. 4, pp. 161–174, 2013, doi: 10.1260/0266-3511.28.3-4.161.

[10] Y. Masson, 'Existence and construction of Chebyshev nets and application to gridshells', Université Paris-Est, Champs-sur-Marne, 2017. Accessed: May 30, 2020. [Online]. Available: https://tel.archives-ouvertes.fr/tel-01676984v2

[11] A. O. Sageman-Furnas, A. Chern, M. Ben-Chen, and A. Vaxman, 'Chebyshev Nets from Commuting PolyVector Fields', *ACM Trans. Graph.*, vol. 38, no. 6, 2019, doi: 10.1145/3355089.3356564.

[12] A. S. Day, 'An Introduction to dynamic relaxation', *The Engineer*, vol. 219, pp. 218–221, 1965.

[13] S. M. L. Adriaenssens, M. R. Barnes, and C. Williams, 'A new analytic and numerical basis for the form-finding and analysis of spline and gridshell structures', in *Computing Developments in Civil and Structural Engineering*, Civil-Comp Press, 1999, pp. 83–91. [Online]. Available: https://researchportal.bath.ac.uk/en/publications/a-new-analytic-and-numerical-basis-for-the-form-finding-and-analy

[14] M. R. Barnes, S. M. L. Adriaenssens, and M. Krupka, 'A novel torsion/bending element for dynamic relaxation modeling', *Computers & Structures*, vol. 119, pp. 60–67, 2013, doi: 10.1016/j.compstruc.2012.12.027.

[15] B. D'Amico, A. Kermani, and H. Zhang, 'A form finding method for post formed timber grid shell structures', Canada, 2014, p. 6. doi: 10.13140/2.1.3949.8888.

[16] L. Du Peloux, F. Tayeb, B. Lefevre, O. Baverel, and J.-F. Caron, 'Formulation of a 4-DoF torsion/bending element for the formfinding of elastic gridshells', in *IASS 2015: Future Visions*, Amsterdam, 2015, p. 16. Accessed: May 30, 2020. [Online]. Available: https://hal.archives-ouvertes.fr/hal-01199049

[17] J. Bessini, C. Lázaro, and S. Monleón, 'A form-finding method based on the geometrically exact rod model for bending-active structures', *Engineering Structures*, vol. 152, pp. 549–558, 2017, doi: 10.1016/j.engstruct.2017.09.045.
[18] M. Sakai, Y. Mori, X. Sun, and K. Takabatake, 'Recent Progress on Mesh-free Particle Methods for Simulations of Multi-phase Flows: A Review', *KONA Powder and Particle Journal*, vol. 37, pp. 132–144, 2020, doi: 10.14356/kona.2020017.
[19] C. Douthe, O. Baverel, and J.-F. Caron, 'Form-finding of a grid shell in composite materials', *J IASS*, vol. 47, p. 10, 2006.
[20] L. Du Peloux, F. Tayeb, J.-F. Caron, and O. Baverel, 'The Ephemeral Cathedral of Créteil : a 350m2 lightweight gridshell structure made of 2 kilometers of GFRP tubes', in *CIGOS 2015: Innovations in Constructions*, Cachan, 2015, p. 10. Accessed: May 30, 2020. [Online]. Available: https://hal.archives-ouvertes.fr/hal-01199044
[21] O. Baverel, J.-F. Caron, F. Tayeb, and L. Du Peloux, 'Gridshells in Composite Materials: Construction of a 300 m2 Forum for the Solidays' Festival in Paris', *Structural Engineering International*, vol. 22, no. 3, pp. 408–414, 2012, doi: 10.2749/101686612X13363869853572.
[22] J. Schlaich and H. Schober, 'Glass Roof for the Hippo House at the Berlin Zoo', *Structural Engineering International*, vol. 7, no. 4, pp. 252–254, 1997, doi: 10.2749/101686697780494581.
[23] C. Douthe, R. Mesnil, H. Orts, and O. Baverel, 'Isoradial meshes: Covering elastic gridshells with planar facets', *Automation in Construction*, vol. 83, pp. 222–236, 2017, doi: 10.1016/j.autcon.2017.08.015.
[24] A. I. Bobenko and Y. B. Suris, *Discrete Differential Geometry : Integrable Structure*. American Mathematical Society, 2008.
[25] J. Natterer, N. Burger, and A. Müller, 'The roof structure "Expodach" at the World Exhibition Hanover 2000', in *Space Structures 5*, Guildford, 2002, pp. 185–193. doi: 10.1680/ss5v1.31739.0020.
[26] C. Pirazzi and Y. Weinand, 'Geodesic Lines on Free-Form Surfaces - Optimized Grids for Timber Rib Shells', 2006, pp. 595–601. Accessed: May 30, 2020. [Online]. Available: https://core.ac.uk/display/147936818?recSetID=
[27] H. Pottmann *et al.*, 'Geodesic Patterns', *ACM Trans. Graph.*, vol. 29, no. 4, p. 10, 2010, doi: 10.1145/1833349.1778780.
[28] M. Rabinovich, T. Hoffmann, and O. Sorkine-Hornung, 'Discrete Geodesic Nets for Modeling Developable Surfaces', *ACM Trans. Graph.*, vol. 37, no. 2, 2018, doi: 10.1145/3180494.
[29] M. Rabinovich, T. Hoffmann, and O. Sorkine-Hornung, 'The Shape Space of Discrete Orthogonal Geodesic Nets', *ACM Trans. Graph.*, vol. 37, no. 6, p. 17, 2018, doi: 10.1145/3272127.3275088.
[30] E. Soriano, R. Sastre, and D. Boixader, 'G-shells: Flat collapsible geodesic mechanisms for gridshells', in *IASS 2019: Form and Force*, Barcelona, 2019, pp. 1894–1901. Accessed: May 30, 2020. [Online]. Available: https://www.ingentaconnect.com/content/iass/piass/2019/00002019/00000011/art00006
[31] S. Pillwein, K. Leimer, M. Birsak, and P. Musialski, 'On Elastic Geodesic Grids and Their Planar to Spatial Deployment', *ACM Trans. Graph.*, vol. 39, no. 4, 2020, doi: 10.1145/3386569.3392490.
[32] H. Wang, D. Pellis, F. Rist, H. Pottmann, K. Matsushita, and C. Müller, 'Discrete Geodesic Parallel Coordinates', *ACM Trans. Graph.*, vol. 38, no. 6, p. 13, 2019, doi: 10.1145/3355089.3356541.
[33] A. E. Voss, 'Ueber diejenigen Flächen, auf denen zwei Schaaren geodätischer Linien ein conjugirtes System bilden.', *Math.-Naturwiss.*, 1888.
[34] W. Wunderlich, 'Zur Differenzengeometrie der Flächen konstanter negativer Krümmung', Wien, 1951, pp. 39–77.
[35] S. E. Taylor, A. Gupta, J. Kirkpatrick, and A. E. Long, 'Testing a novel flexible concrete arch system', presented at the Advanced Composites in Construction, Bath, 2007. Accessed: Sep. 15, 2020. [Online]. Available: https://citeseerx.ist.psu.edu/viewdoc/summary?doi=10.1.1.1075.5870

[36] H. Pottmann, Y. Liu, J. Wallner, A. I. Bobenko, and W. Wang, 'Geometry of Multi-Layer Freeform Structures for Architecture', *ACM Trans. Graph.*, vol. 26, no. 3, 2007, doi: 10.1145/1276377.1276458.
[37] P. Romon, *Introduction à la géométrie différentielle discrète*. Ellipses, 2013. [Online]. Available: https://hal.archives-ouvertes.fr/hal-00926137
[38] U. Pinkall, 'Selected topics in Discrete Differential Geometry and Visualization', Beijing, 2009. [Online]. Available: https://www3.math.tu-berlin.de/geometrie/gpspde/2009DDGandVis/iddg.pdf
[39] W. K. Schief, A. I. Bobenko, and T. Hoffmann, 'On the Integrability of Infinitesimal and Finite Deformations of Polyhedral Surfaces', in *Discrete Differential Geometry*, A. I. Bobenko, J. M. Sullivan, P. Schröder, and G. M. Ziegler, Eds. Basel: Birkhäuser Basel, 2008, pp. 67–93. [Online]. Available: https://doi.org/10.1007/978-3-7643-8621-4_4
[40] J.-F. Frenet, 'Sur les courbes à double courbure', *Journal de Mathématiques Pures et Appliquées*, vol. 17, no. 1, pp. 437–447, 1852.
[41] R. Sauer, *Differenzengeometrie*. Springer Verlag, 1970. [Online]. Available: https://doi.org/10.1007/978-3-642-86411-7
[42] O. Sorkine-Hornung, D. Cohen-Or, Y. Lipman, M. Alexa, C. Rössl, and H. P. Seidel, 'Laplacian Surface Editing', in *Eurographics Symposium on Geometry Processing 2004*, 2004, pp. 175–184. doi: 10.1145/1057432.1057456.
[43] M. Kilian, N. J. Mitra, and H. Pottmann, 'Geometric Modeling in Shape Space', *ACM Trans. Graph.*, vol. 26, no. 3, pp. 64–71, 2007, doi: 10.1145/1276377.1276457.
[44] M. Botsch and O. Sorkine-Hornung, 'On Linear Variational Surface Deformation Methods', *IEEE Trans. Vis Comput. Graph.*, vol. 14, no. 1, pp. 213–230, 2008, doi: 10.1109/TVCG.2007.1054.
[45] Y.-L. Yang, Y.-J. Yang, H. Pottmann, and N. J. Mitra, 'Shape Space Exploration of Constrained Meshes', *ACM Trans. Graph.*, vol. 30, no. 6, p. 12, 2011, doi: 10.1145/2070781.2024158.
[46] Y. Liu, H. Pottmann, J. Wallner, Y.-L. Yang, and W. Wang, 'Geometric Modeling with Conical Meshes and Developable Surfaces', *ACM Trans. Graph.*, vol. 25, no. 3, pp. 681--689, 2006, doi: 10.1145/1141911.1141941.
[47] S. Bouaziz, M. M. Deuss, Y. Schwartzburg, T. Weise, and M. Pauly, 'Shape-Up: Shaping Discrete Geometry with Projections', in *Eurographics Symposium on Geometry Processing 2012*, Tallinn, 2012, vol. 31, pp. 1657--1667. doi: 10.1111/j.1467-8659.2012.03171.x.
[48] A. Vaxman, 'A Projective Framework for Polyhedral Mesh Modelling', *Computer Graphics Forum*, vol. 33, no. 8, pp. 121–131, 2014, doi: 10.1111/cgf.12405.
[49] R. Poranne, R. Chen, and C. Gotsman, 'On Linear Spaces of Polyhedral Meshes', *IEEE Trans. Vis Comput. Graph.*, vol. 21, no. 5, pp. 652–662, 2015, doi: 10.1109/TVCG.2014.2388205.
[50] R. Mesnil, C. Douthe, O. Baverel, and B. Léger, 'Marionette Meshes: Modelling free-form architecture with planar facets', *International Journal of Space Structures*, vol. 32, no. 3–4, pp. 184–198, 2017, doi: 10.1177/0266351117738379.
[51] C. Douthe *et al.*, 'Design and construction of a shell-nexorade hybrid timber structure', presented at the International Association for Shell and Spatial Structures Symposium, Boston, 2018. [Online]. Available: https://hal-enpc.archives-ouvertes.fr/hal-01852280
[52] T. Tachi, 'Freeform Rigid-Foldable Structure using Bidirectionally Flat-Foldable Planar Quadrilateral Mesh', 2010, pp. 87–102. doi: 10.1007/978-3-7091-0309-8_6.
[53] T. Mitchell, A. Mazurek, C. Hartz, M. Miki, and W. Baker, 'Structural Applications of the Graphic Statics and StaticKinematic Dualities: Rigid Origami, Self-Centering Cable Nets, and Linkage Meshes', presented at the International Association for Shell and Spatial Structures Symposium, Boston, 2018. Accessed: Jun. 15, 2020. [Online]. Available: https://www.ingentaconnect.com/content/iass/piass/2018/00002018/00000016/art00010
[54] E. Ghys, 'Sur la coupe des vetements: variation autour d'un thme de Tchebyshev', *L'Enseignement Mathematique*, vol. 57, no. 2, pp. 165–208, 2011.

[55] U. Pinkall, ‘Designing Cylinders with Constant Negative Curvature’, in *Discrete Differential Geometry*, A. I. Bobenko, J. M. Sullivan, P. Schröder, and G. M. Ziegler, Eds. Birkhäuser Basel, 2008, pp. 55–66. [Online]. Available: https://doi.org/10.1007/978-3-7643-8621-4_3

[56] R. Mesnil, C. Douthe, O. Baverel, and B. Léger, ‘Morphogenesis of surfaces with planar lines of curvature and application to architectural design’, *Automation in Construction*, vol. 95, pp. 129–141, 2018, doi: 10.1016/j.autcon.2018.08.007.

[57] D. Rutten, ‘Galapagos: On the Logic and Limitations of Generic Solvers’, *Architectural Design*, vol. 83, no. 2, pp. 132–135, 2013, doi: 10.1002/ad.1568.

APPENDIX: COMPUTATION OF A CHEBYSHEV NET $\mathcal{S}^2$

Literature is filled with strategies for generating Chebyshev nets on general surfaces. They are based on geometrical considerations or optimisation principles, which are computationally heavy. In [38] a specific method is explained to generate Chebyshev nets on the unit sphere using unit quaternions. The embedding in the 4D space of quaternions allows to build the Chebyshev net from simple addition and multiplication.

Considering v_a, v_b, v_c and v_d the vertices of a spherical parallelogram contained in a hemisphere of the unit sphere $\mathcal{S}^2$ (Figure 22), the following relation holds:

$$(\mathrm{v}_a + \mathrm{v}_c) \times (\mathrm{v}_b + \mathrm{v}_d) = 0,$$

which is equivalent to stating that the rotation about the axis $(\mathrm{v}_a + \mathrm{v}_c)$ or $(\mathrm{v}_b + \mathrm{v}_d)$ of an angle of π, transforms the spherical parallelogram to itself. The position of the vertices v_a and v_c, and v_b and v_d are inverted. Thus, if the vertices v_a, v_b and v_d are known, v_c can be computed from v_a by rotation of an angle π around the axis $(\mathrm{v}_b + \mathrm{v}_d)$.

The space of unit quaternions is then used to compute this rotation in a straightforward way. Let's consider the rotation of a point $\mathrm{p} = (p_x, p_y, p_z)$ around the unitized axis $\mathrm{d} = (d_x, d_y, d_z)$ of an angle α. The unit rotation quaternion is defined by:

$$\mathrm{q} = \left(cos\left(\frac{\alpha}{2}\right), sin\left(\frac{\alpha}{2}\right) \cdot d_x, sin\left(\frac{\alpha}{2}\right) \cdot d_y, sin\left(\frac{\alpha}{2}\right) \cdot d_z\right).$$

Using the identification between the Euclidean space $\mathbb{R}^3 = \{(x, y, z); x, y, z \in \mathbb{R}\}$ and the space of imaginary quaternions $\mathbb{H} = \{(0, x, y, z); x, y, z \in \mathbb{R}\}$, the resulting point of the rotation is computed as:

$$\mathrm{r} = \mathrm{q} \cdot \mathrm{p} \cdot \mathrm{q}^{-1}.$$

Using this formula with:

$$\mathrm{p} = \mathrm{v}_a, \qquad \mathrm{d} = \frac{\mathrm{v}_b + \mathrm{v}_d}{\|\mathrm{v}_b + \mathrm{v}_d\|}, \qquad \alpha = \pi,$$

the resulting r, or more precisely its imaginary, is the position of v_c.

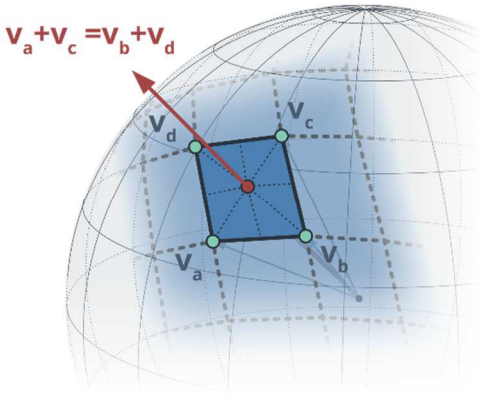

Figure 22: Spherical parallelogram and the rotation axis mapping the quad to itself through a rotation of an angle π